Technical Document 1550
June 1989

Mathematical Analysis of Scissor Lifts

H. M. Spackman

NAVAL OCEAN SYSTEMS CENTER

San Diego, California 92152–5000

E. G. SCHWEIZER, CAPT, USN
Commander

R. M. HILLYER
Technical Director

ADMINISTRATIVE INFORMATION

This work was performed for the U.S. Marine Corps, Development/Education Command, Quantico, VA 22134, under program element number 0603635M and agency accession number DN308 274. The work was performed by the Advanced Technology Development Branch, Code 612, Naval Ocean Systems Center, San Diego, CA 92152–5000.

Released by
R. E. Glass, Head
Advanced Technology
Development Branch

Under authority of
D. W. Murphy, Head
Advanced Systems
Division

FS

REPORT DOCUMENTATION PAGE

1a. REPORT SECURITY CLASSIFICATION UNCLASSIFIED	1b. RESTRICTIVE MARKINGS
2a. SECURITY CLASSIFICATION AUTHORITY	3. DISTRIBUTION/AVAILABILITY OF REPORT Approved for public release; distribution is unlimited.
2b. DECLASSIFICATION/DOWNGRADING SCHEDULE	
4. PERFORMING ORGANIZATION REPORT NUMBER(S) NOSC TD 1550	5. MONITORING ORGANIZATION REPORT NUMBER(S)
6a. NAME OF PERFORMING ORGANIZATION Naval Ocean Systems Center 6b. OFFICE SYMBOL (if applicable) Code 612	7a. NAME OF MONITORING ORGANIZATION
6c. ADDRESS (City, State and ZIP Code) San Diego, California 92152-5000	7b. ADDRESS (City, State and ZIP Code)
8a. NAME OF FUNDING/SPONSORING ORGANIZATION U.S. Marine Corps 8b. OFFICE SYMBOL (if applicable)	9. PROCUREMENT INSTRUMENT IDENTIFICATION NUMBER
8c. ADDRESS (City, State and ZIP Code) Development/Education Command Quantico, VA 22134	10. SOURCE OF FUNDING NUMBERS PROGRAM ELEMENT NO. 0603635M; PROJECT NO. CH58; TASK NO.; AGENCY ACCESSION NO. DN308 274

11. TITLE (include Security Classification)

Mathematical Analysis of Scissor Lifts

12. PERSONAL AUTHOR(S)

H. M. Spackman

13a. TYPE OF REPORT	13b. TIME COVERED	14. DATE OF REPORT (Year, Month, Day)	15. PAGE COUNT
Final	FROM TO	June 1989	63

16. SUPPLEMENTARY NOTATION

17. COSATI CODES			18. SUBJECT TERMS (Continue on reverse if necessary and identify by block number)
FIELD	GROUP	SUB-GROUP	
			scissor lift, actuator placement, member cross-section

19. ABSTRACT (Continue on reverse if necessary and identify by block number)

This document presents mathematical techniques for analyzing reaction forces in scissor lifts. It also presents several design issues including actuator placement, member cross-section, and rigidity.

20. DISTRIBUTION/AVAILABILITY OF ABSTRACT	21. ABSTRACT SECURITY CLASSIFICATION
☐ UNCLASSIFIED/UNLIMITED ☒ SAME AS RPT ☐ DTIC USERS	UNCLASSIFIED

22a. NAME OF RESPONSIBLE INDIVIDUAL	22b. TELEPHONE (include Area Code)	22c. OFFICE SYMBOL
H. M. Spackman	(619) 553-6110	Code 612

DD FORM 1473, 84 JAN

83 APR EDITION MAY BE USED UNTIL EXHAUSTED
ALL OTHER EDITIONS ARE OBSOLETE

CONTENTS

FIGURES

FIGURES (continued)

TABLE

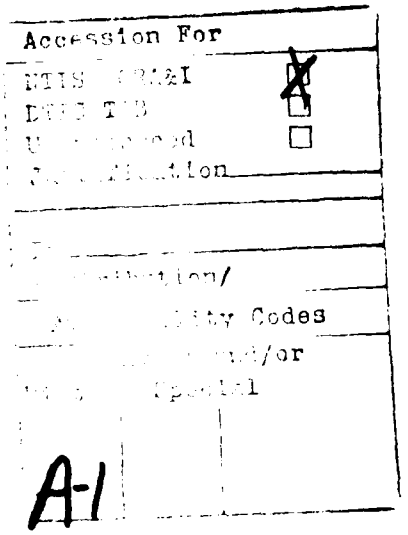

1.0 INTRODUCTION

The purpose of this document is to present mathematical equations for analyzing reaction forces in scissor lifts and to discuss several design issues including actuator placement, and strength and rigidity. In section 2.0 the nomenclature is presented. In section 3.1 equations are derived for the scissor members whose reaction forces are not affected by the actuators. In section 3.2, equations for calulating the actuator forces directly are given. In section 4.0 the equations from sections 3.1 and 3.2 are combined into a single method of determining the reaction forces throughout the lift. Forces obtained from this analysis can be used in selecting the appropriate material and cross-section of the scissor members, and to select suitable actuators. In the remaining sections the design issues listed above are discussed.

2.0 NOMENCLATURE

Figure 1 shows an *n*-level scissor lift with the six possible applied loads. The letter H is used instead of F for the linear forces in order to avoid confusion with later terminology. Notice that H_x and H_z act in the positive x and z directions, respectively, while H_y acts in the negative y direction. The direction of H_y was selected to correspond with loads normally encountered. At each joint there are also six possible reaction forces and moments. In order to distinguish between joints, the nomenclature shown in figure 2 will be used. The subscripts L, R, F, B, and M are used to denote left, right, front, back and middle, respectively. This system of subscripting was selected because the reaction forces are usually symmetric allowing some of the subscripts to be dropped. One slight inconsistency in this nomenclature is the M subscript. All other subscripts come in pairs, and to be totally consistent one more subscript could have been included to denote bottom. The reasons for omitting this subscript are that symmetry never exists between the bottom and middle joints, and the bottom joints already have an excessive number of subscripts. There are cases in the paper where the L, R, F, and B subscripts are all dropped from the reaction forces at the bottom of the scissor resulting in X_i, Y_i, or Z_i. The reader may mistakenly assume that the equations for X_i, Y_i, and Z_i also apply to the middle joints. This is not true. X_i, Y_i, and Z_i apply only to the bottom joints. The M subscript is never dropped.

Notice that the reaction forces at the top of the i and i–1 scissors are not shown in figure 2. These forces are omitted because they are equal and opposite the forces at the bottom of the previous scissor, and therefore are not unique. Also notice that none of the possible reaction moments at the joints are shown. The moment about the z axis is omitted because the joints are assumed to be frictionless. The reason this assumption is possible is because the radius through which the friction forces act is small and, if the joints are lubricated, the coefficient of friction is small. The reaction moments about the x and y axis' are zero for loads applied in the x-y plane. These loads include H_x, H_y, and M_z. It is believed that they are also negligible for the out-of-plane loads M_x, M_y, and H_z especially if cross-bracing is used.

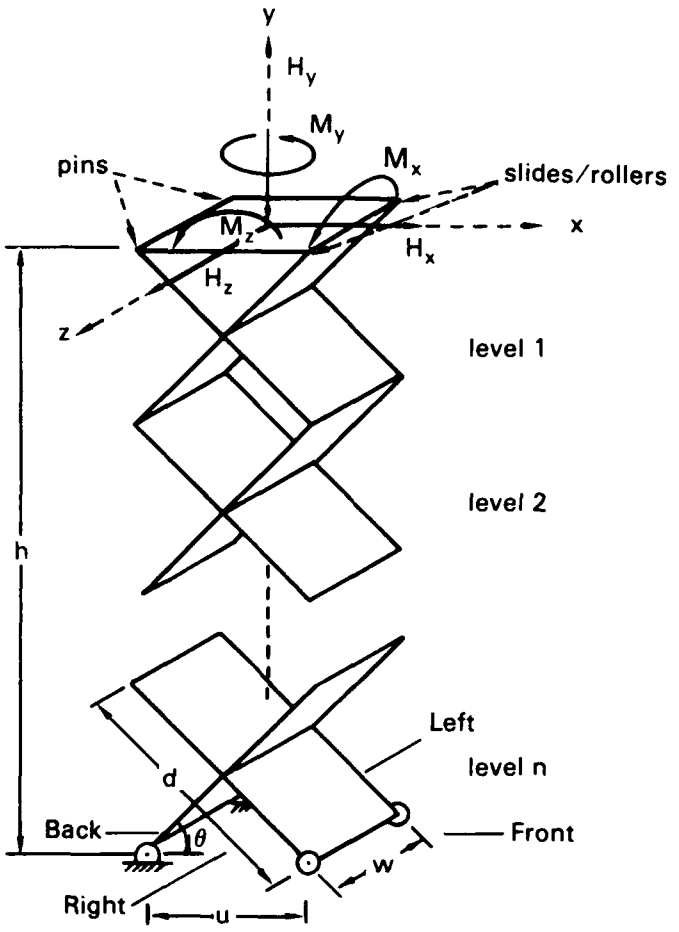

Figure 1. Nomenclature: applied loads and scissor lift dimensions.

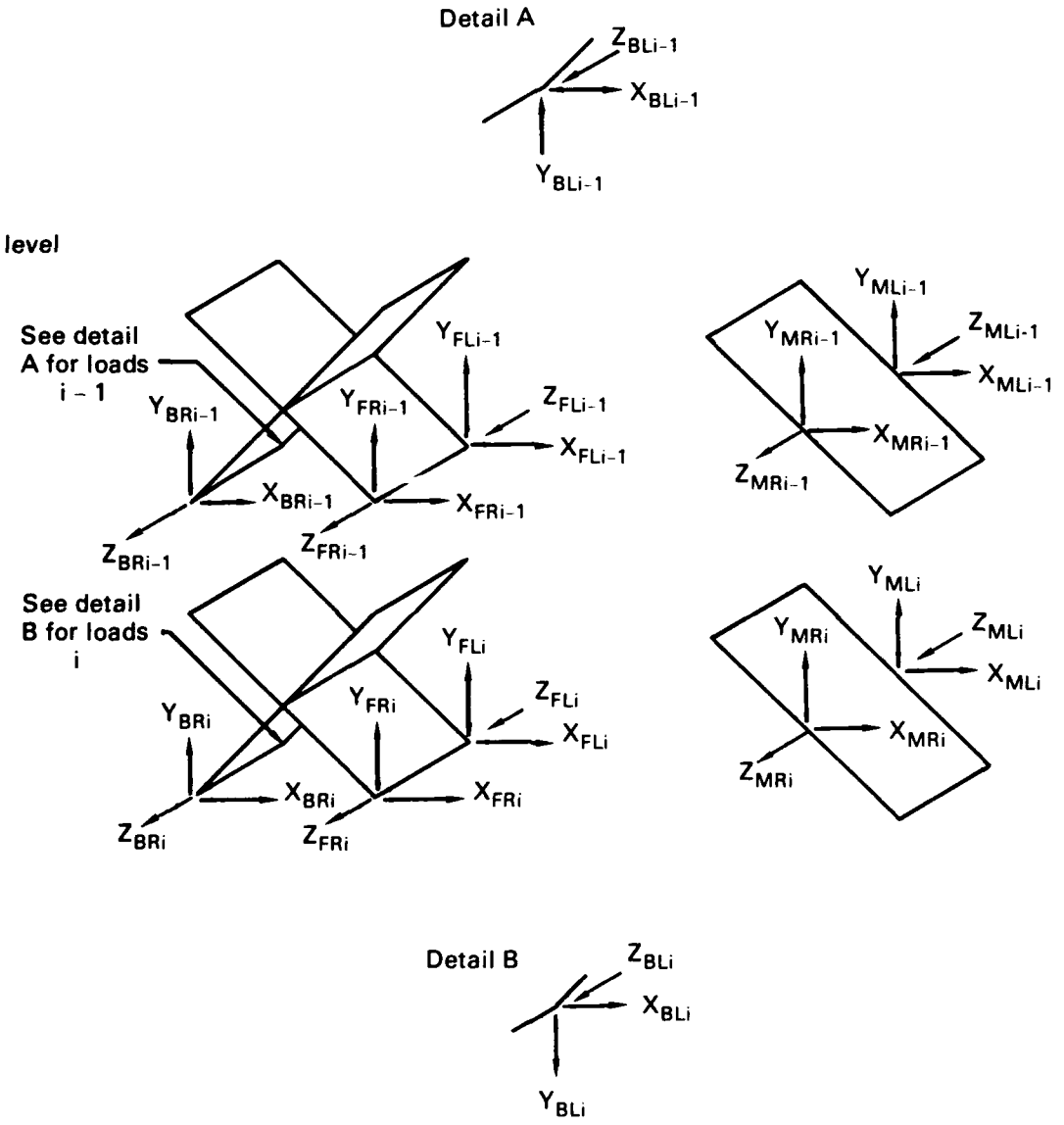

Reaction Force	Location	Level
X-Force in pos. x dir	F-front	1 thru n
Y-Force in pos. y dir	B-back	
Z-Force in pos. z dir	L-left	
	R-right	
	M-middle	

Figure 2. Nomenclature: reaction forces.

3.0 GENERAL SCISSOR LIFT EQUATIONS

An n-level scissor lift with a single actuator in the i and i+1 levels is shown in figure 3a. One possible way of calculating the reaction forces throughout the lift is to begin at the top of the lift where the applied loads are known, and, using equations of static equilibrium, solve for the reaction forces in the first scissor (level 1). The forces at the top of the second scissor are now known since they are equal and opposite the forces at the bottom of level 1, and the forces in the second level can now be calculated. This process continues to level i. At this level there are more unknowns than equations because the actuator adds an unknown variable. The analysis now shifts to the bottom of the lift. The reaction forces at the bottom of the lift can be found by doing a freebody analysis of the entire lift. Once the forces at the bottom of the lift are known, the reaction forces from level n to the bottom of level i+1 can be calculated. Now that the forces are known at the top of level i and at the bottom of level i+1, the remaining reaction forces can be determined using equations of static equilibrium.

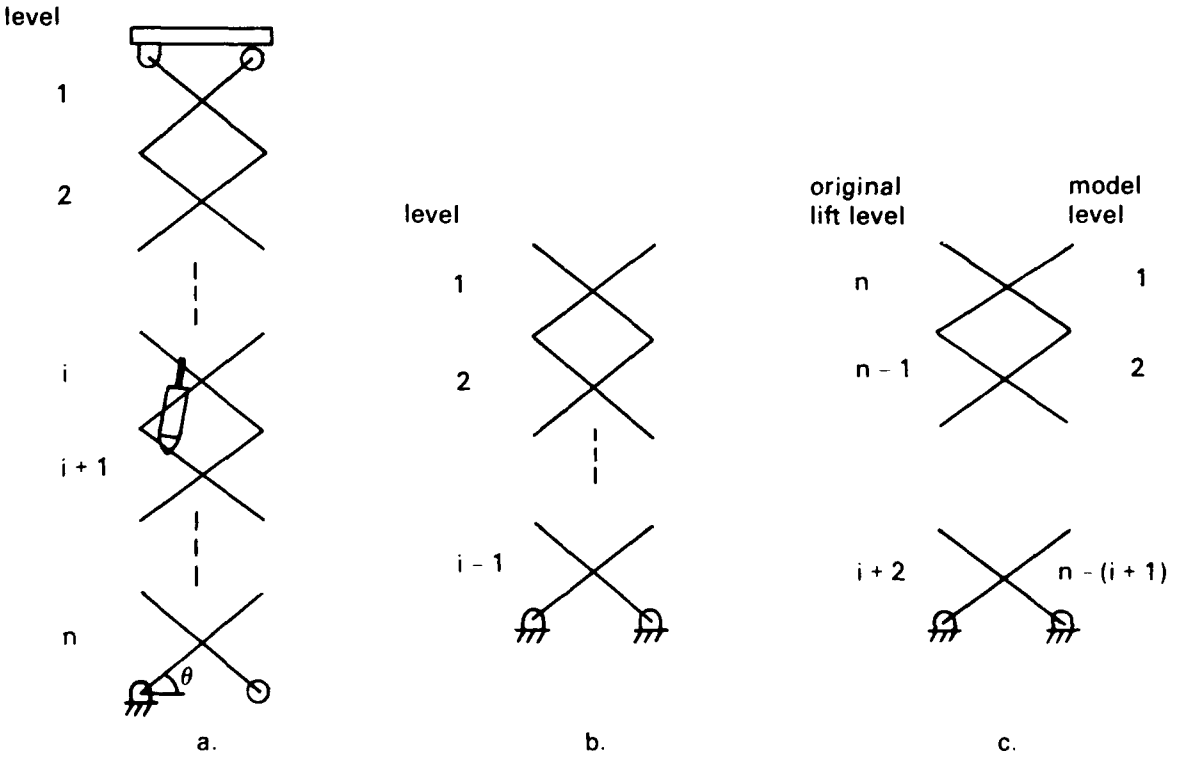

Figure 3. Scissor lift models.

This method of solution is almost impossible to do by hand because any error will be carried on to later calculations. Also the number of calculations is overwhelming. It is therefore desirable to find a simpler method of analysis. Before developing this alternate method, two critical observations about the lift are necessary. First, notice that the reaction forces in levels i through i-1 and in levels i+2 through n are completely unaffected by the placement of the actuator as long as it is confined within the i and i+1 levels. In fact, the scissor members in levels 1 through i-1 can be modeled as a scissor structure that has no actuators and is pinned to "ground" at all four bottom joints as shown in figure 3b. This structure will be referred to as "the basic scissor structure" throughout this paper. This thought process can be continued by considering levels i+2 through n. Notice that these members meet the criteria of a basic scissor structure except that the structure is upside down. This portion of the lift can therefore be modeled as the basic scissor structure shown in figure 3c. In this model the lift will have negative weight. The loads at the top of this model are easily determined by doing a freebody analysis on the entire lift. The second critical observation is that if frictional losses are assumed to be negligible, then the principle of conservation of energy applies. This allows the actuator forces to be calculated directly.

In section 3.1 general equations that give the reaction forces in the basic scissor structure are derived. In section 3.2 equations for calculating the actuator forces are derived. A discussion about the proper application of these formulas is given in section 4.0.

3.1 EQUATIONS FOR THE BASIC SCISSOR STRUCTURE

The possible loads on a scissor lift were illustrated in figure 1. In this section reaction force equations for the basic scissor structure are derived separately for each load.

3.1.1 Load 1: Centered Load in the Negative y Direction

The first load that is considered is H_y. This load can be made more general by including the distributed weight of the scissor lift. Let B equal the weight of the lift. If the lift is on an inclined surface then the weight of the lift will have components in the x, y, and z directions which will be denoted by B_x, B_y, and B_z, respectively. Positive B_y is in the negative y direction whereas positive B_x and B_z are in the positive x and z directions, respectively. Let H_{y0} equal the applied load at the top of the lift, and let H_{yi} equal H_{y0} plus the weight of the lift in the negative y direction up to and including level i. If all the levels have the same weight and this weight is denoted by b_y then,

$$H_{yi} = H_{y0} + ib_y \tag{1}$$

where,

$$b_y = B_y / n .$$

This loading condition is shown in figure 4. A platform is shown at the top of the structure but the type of connection between the platform and the top joints is not shown. It is assumed that either the front or back joints are attached via slides/rollers and the other via pins. The joints that are attached via slides/rollers cannot support any load in the x direction. This assumption is used for all loads except for load 6.

Because the load is centered and vertical, the reaction forces on the left side of the lift are identical to the right side. Therefore, only one side of the lift needs to be analyzed, and the L and R subscripts can be dropped. Also, if the scissor lift is rotated 180 degrees about the y axis, the problem is exactly the same. This implies that the reaction forces are symmetric about the y-z plane. In mathematical terms this means that

$$Y_{Bi} = Y_{Fi} = Y_i ,$$

$$X_{Fi} = - X_{Bi} ,$$

$$Y_{Mi} = 0 .$$

Figure 5a shows a freebody diagram of the right side of the lift. The equation for Y_i is derived using principles of static equilibrium as follows.

From figure 5a,

$$\Sigma F_Y = 0,$$

$$2 Y_i - 2 \frac{H_{y0}}{4} - \frac{ib_y}{2} = 0 ,$$

$$Y_i = \frac{H_{y0} + ib_y}{4} ,$$

$$= \frac{H_{yi}}{4} .$$

The reaction forces acting on level i are shown in figures 5b and 5c. Referring to figure 5c,

$$\Sigma M_p = 0,$$

$$-X_{Bi} \frac{d}{2} \sin\theta + \frac{H_{yi}}{4} \frac{d}{2} \cos\theta + \frac{H_{yi-1}}{4} \frac{d}{2} \cos\theta + X_{Bi-1} \frac{d}{2} \sin\theta = 0 ,$$

$$X_{Bi} - X_{Bi-1} = \frac{H_{yi} + H_{yi-1}}{4 \tan\theta} .$$

This equation only gives the change of X_B with each succeeding level. In order to find the general equation for X_{Bi} let

$$f(i) = \frac{H_{yi} + H_{yi-1}}{4 \tan\theta} .$$

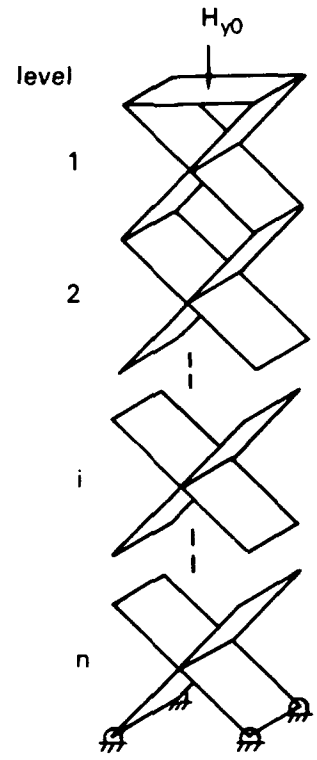

Figure 4. Basic scissor structure with load applied in the negative y direction.

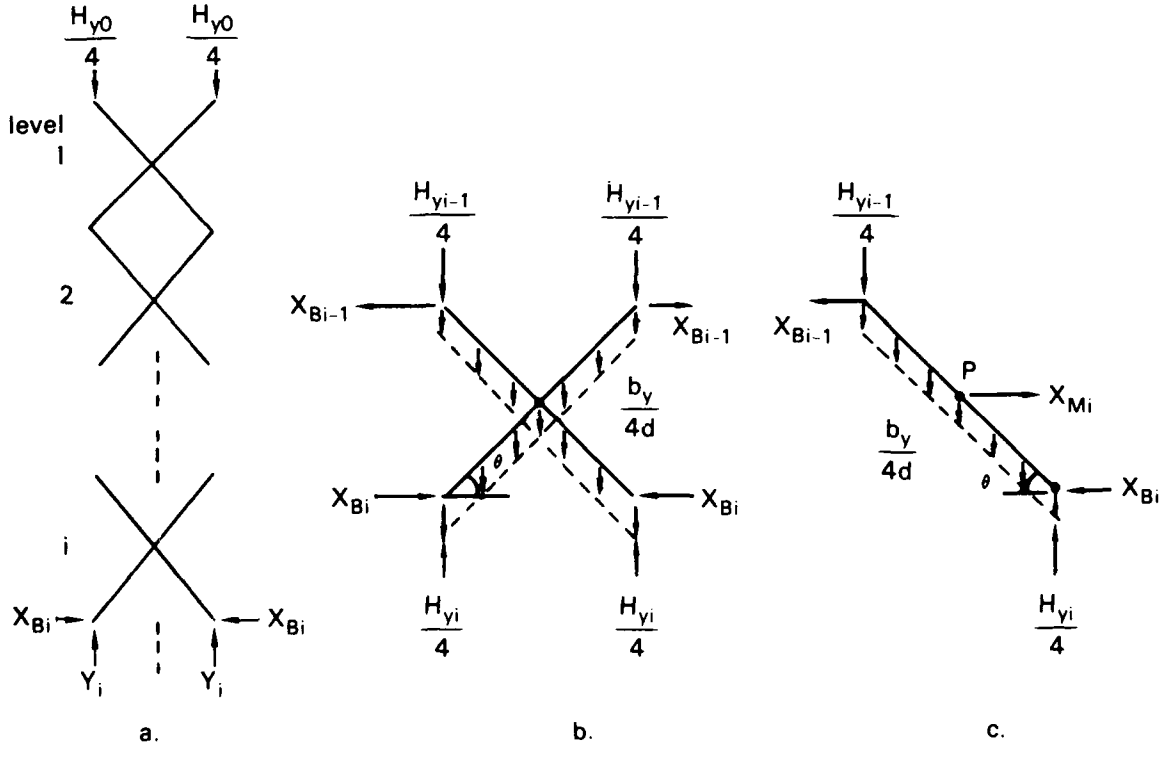

Figure 5. Freebody diagrams for load applied in the negative y direction.

If the equation is written for all the levels up to i, the following set of equations is obtained.

$$X_{Bi} - X_{Bi-1} = f(i) ,$$

$$X_{Bi-1} - X_{Bi-2} = f(i-1) ,$$

$$\vdots$$

$$X_{B1} - X_{B0} = f(1) .$$

Notice that if the above equations are added together, all of the terms on the left of the equal sign cancel except for X_{Bi} and X_{B0}. Performing the addition results in

$$X_{Bi} - X_{B0} = \sum_{k=1}^{i} f(k) ,$$

$$= \sum_{k=1}^{i} \frac{H_{yk} + H_{yk-1}}{4 \tan \theta} .$$

And from equation 1

$$X_{Bi} - X_{B0} = \sum_{k=1}^{i} \frac{H_{y0} + kb_y + H_{y0} + (k-1) b_y}{4 \tan \theta} ,$$

$$= \sum_{k=1}^{i} \left(\frac{H_{y0}}{2 \tan \theta} + \frac{(2k-1) b_y}{4 \tan \theta} \right) ,$$

$$= \frac{iH_{y0}}{2 \tan \theta} + \frac{b_y}{4 \tan \theta} \sum_{k=1}^{i} (2k-1) ,$$

$$= \frac{iH_{y0}}{2 \tan \theta} + \frac{b_y}{4 \tan \theta} \left(2 \sum_{k=1}^{i} k - \sum_{k=1}^{i} 1 \right) ,$$

$$= \frac{iH_{y0}}{2 \tan \theta} + \frac{b_y}{4 \tan \theta} \left(2 \frac{i(i+1)}{2} - i \right) ,$$

$$= \frac{iH_{y0}}{2 \tan \theta} + \frac{i^2 b_y}{4 \tan \theta} ,$$

$$= \left(H_{y0} + \frac{ib_y}{2} \right) \frac{i}{2 \tan \theta} .$$

Since one pair of joints at the top of the lift is connected to rollers, X_{B0} equals zero and

$$X_{Bi} = \left(H_{y0} + \frac{ib_y}{2}\right) \frac{i}{2 \tan \theta} .$$

Solving now for X_{Mi} from figure 5c

$$\Sigma F_x = 0,$$

$$X_{Mi} - X_{Bi} - X_{Bi-1} = 0 ,$$

$$X_{Mi} = X_{Bi} + X_{Bi-1} ,$$

$$= \left(\frac{iH_{y0}}{2 \tan \theta} + \frac{i^2 b_y}{4 \tan \theta}\right) + \left(\frac{(i-1) H_{y0}}{2 \tan \theta} + \frac{(i-1)^2 b_y}{4 \tan \theta}\right),$$

$$= \frac{(2i-1) H_{y0}}{2 \tan \theta} + \frac{(2i^2 - 2i + 1) b_y}{4 \tan \theta} .$$

In summary

$$X_{Bi} = -X_{Fi} = \left(H_{y0} + \frac{ib_y}{2}\right) \frac{i}{2 \tan \theta}$$

$$Y_i = \frac{H_{y0} + ib_y}{4} ,$$

$$X_{Mi} = \frac{(2i-1) H_{y0}}{2 \tan \theta} + \frac{(2i^2 - 2i + 1) b_y}{4 \tan \theta} ,$$

$$Y_{Mi} = 0 .$$

$$Z_i = Z_{Mi} = 0$$

It should be noted that the reaction loads are completely independent of the length of the scissor members and only depend on the applied load (including the distributed weight of the lift) and the angle of the scissor members from horizontal.

3.1.2 Load 2: Moment About the z Axis

This loading condition is shown in figure 6a. In order to analyze this case, a critical observation needs to be made. Typically, the front or back joints at the top of the lift are pinned to the platform, and the other pair is attached via slides/rollers. Because of this, only the pinned pair can support loads in the x direction. Since the applied load is a moment and has no net linear force, and because of symmetry, the resulting forces in the x direction at the pinned joints are zero. A moment can be represented by a force couple where the two forces are equal and opposite but not colinear. Because the forces on the top

joints of the lift can have no x component, the couple used to represent the moment must be composed of forces acting in the y direction as shown in figure 6b. The equation relating F to M_z is

$$M_z = F\, d \cos\theta\,,$$

$$F = \frac{M_z}{d \cos\theta}\,. \tag{2}$$

Since the load acts in the x-y plane the reaction forces on the right side of the platform are identical to the left side, and the L and R subscripts can be dropped. The loads on one side of level 1 are shown in figure 7.

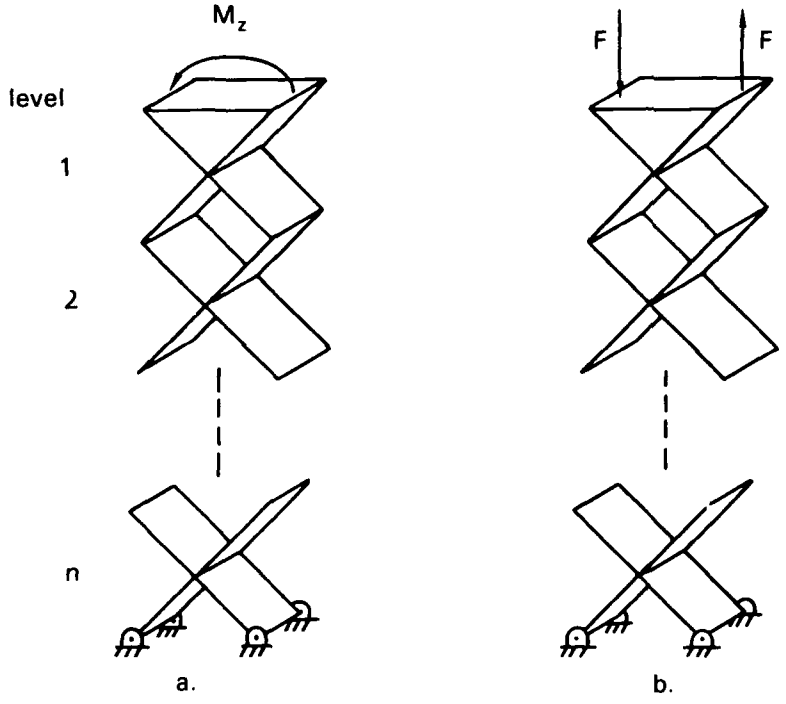

Figure 6. Basic scissor structure with a moment about the z axis.

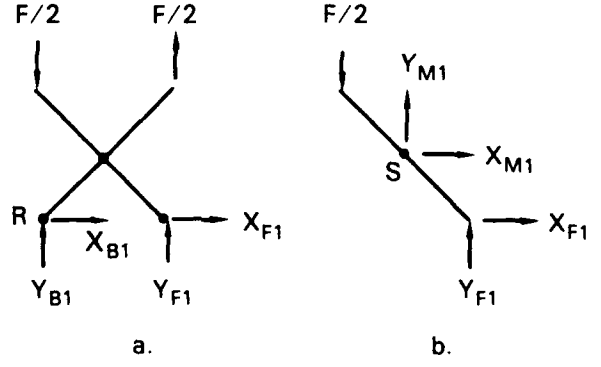

Figure 7. Freebody diagrams for applied moment about the z axis.

Referring to figure 7,

$$\Sigma M_R = 0$$

$$\frac{F}{2}\, d \cos\theta + Y_{F1}\, d \cos\theta = 0$$

$$Y_{F1} = -\frac{F}{2}.$$

$$\Sigma F_y = 0$$

$$Y_{B1} + Y_{F1} + \frac{F}{2} - \frac{F}{2} = 0$$

$$Y_{B1} = -Y_{F1}$$

$$= \frac{F}{2}.$$

$$\Sigma M_s = 0$$

$$\frac{F}{2}\,\frac{d}{2} \cos\theta + Y_{F1}\,\frac{d}{2} \cos\theta + X_{F1}\,\frac{d}{2} \sin\theta = 0$$

$$X_{F1} = 0.$$

$$\Sigma F_x = 0$$

$$X_{B1} + X_{F1} = 0$$

$$X_{B1} = 0.$$

The above equations show that the forces at the top of level two are identical to the loads at the top of level one. This implies that reaction forces at all levels are the same as level one, and only the forces at level 1 need to be determined. The remaining equations are derived as follows.

$$\Sigma F_y = 0$$

$$-\frac{F}{2} + Y_{F1} + Y_{M1} = 0$$

$$Y_{M1} = \frac{F}{2} - Y_{F1}$$

$$= F.$$

$$\Sigma F_x = 0$$

$$X_{M1} + X_{F1} = 0$$

$$X_{M1} = -X_{F1}$$

$$= 0 .$$

Since the reaction forces are the same for all levels, the general equations are given by substituting i for 1 in the subscripts. The equations can also be expressed in terms of the applied moment M_z by substituting $M_z/(d \cos \theta)$ for F (see equation 2).

The final result is

$$Y_{Bi} = \frac{F}{2} = \frac{M_z}{2\, d \cos \theta}$$

$$Y_{Fi} = -\frac{F}{2} = -\frac{M_z}{2\, d \cos \theta}$$

$$Y_{Mi} = F = \frac{M_z}{d \cos \theta}$$

$$X_{Mi} = X_{Bi} = X_{Fi} = 0 .$$

$$Z_i = Z_{Mi} = 0$$

3.1.3 Load 3: Centered Horizontal Load in the Positive x Direction

As with the analysis for a load applied in the negative direction, the analysis for this load can be made more general by including the weight of the lift in the x direction. Let H_{x0} equal the load applied at the top of the lift and let H_{xi} equal H_{x0} plus the weight of the lift in the x direction up to and including level i. If all levels have the same weight and the weight of one level equals b, then

$$H_{xi} = H_{x0} + ib_x ,$$

where

$$b_x = \frac{B_x}{n} .$$

A basic scissor structure with this load is shown in figure 8. Again, because of symmetry, the L and R subscripts can be dropped. The reaction forces in the x direction in this case depend on whether the back or the front joints at the top of the scissor lift are pinned. The reaction forces for both cases will be analyzed.

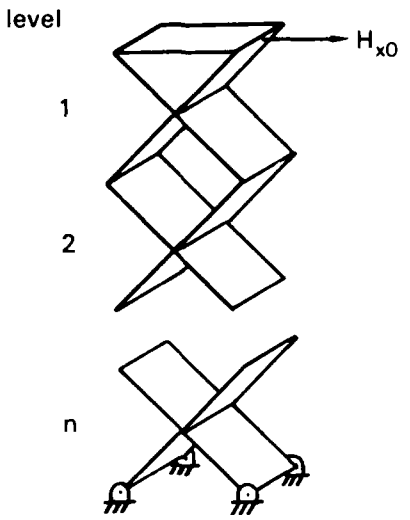

Figure 8. Basic scissor structure with load applied in the positive x direction.

Back Joints Pinned

Assuming the back joints are pinned, the freebody diagram of the lift up to level i is as shown in figure 9a. Y_{Bi} and Y_{Fi} are found as follows.

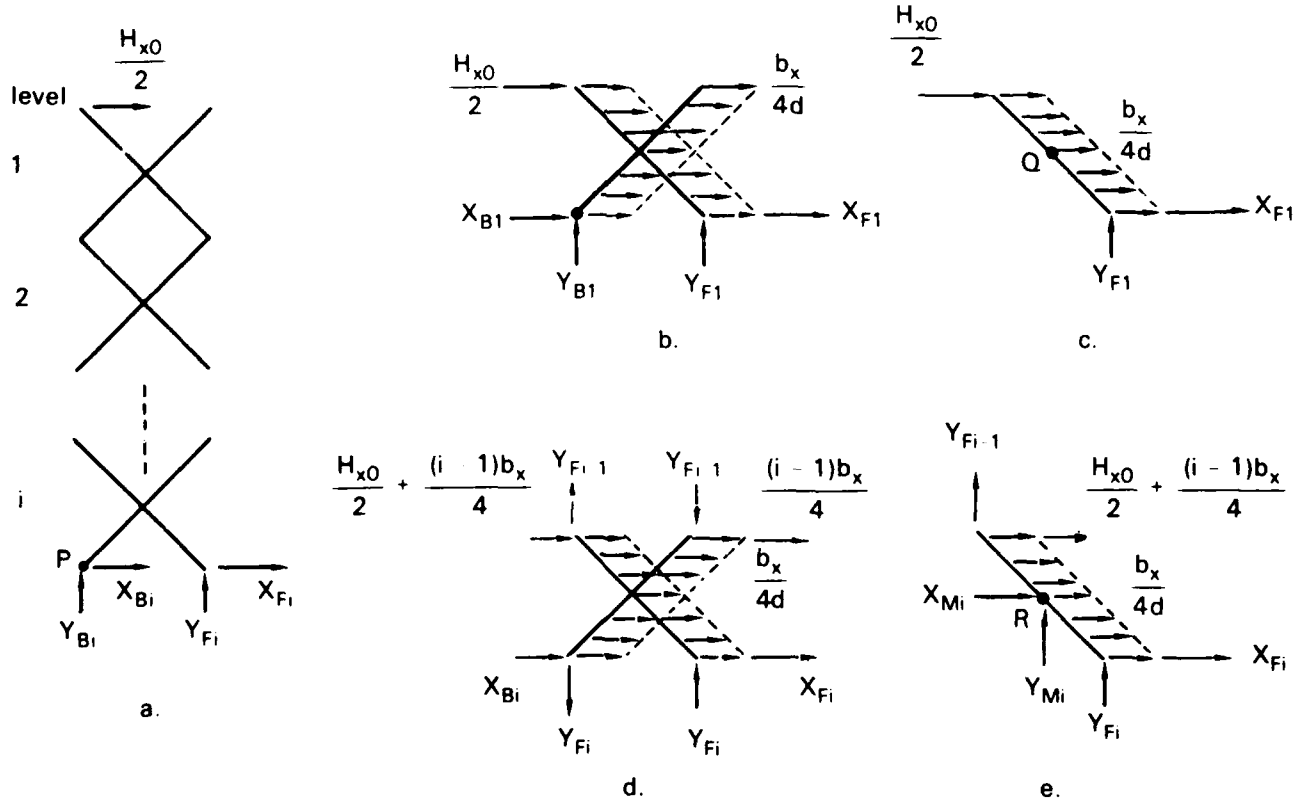

Figure 9. Freebody diagrams for load applied in x direction with the back joints pinned.

$$\Sigma M_p = 0$$

$$Y_{Fi}\, d \cos\theta - \frac{H_{x0}}{2}\, id \sin\theta - \frac{ib_x}{2}\,\frac{id}{2}\sin\theta = 0$$

$$Y_{Fi} - \frac{H_{x0}}{2}\, i \tan\theta - \frac{b_x}{4}\, i^2 \tan\theta = 0$$

$$Y_{Fi} = \left(H_{x0} + \frac{ib_x}{2}\right)\frac{i \tan\theta}{2} . \qquad (3)$$

$$\Sigma F_y = 0$$

$$Y_{Bi} = - Y_{Fi} = \left(H_{x0} + \frac{ib_x}{2}\right)\frac{i \tan\theta}{2} . \qquad (4)$$

The forces on level one are shown in figure 9b and 9c. From figure 9c

$$\Sigma M_Q = 0$$

$$X_{F1}\,\frac{d}{2}\sin\theta - \frac{H_{x0}}{2}\,\frac{d}{2}\sin\theta + Y_{F1}\,\frac{d}{2}\cos\theta = 0$$

$$X_{F1} - \frac{H_{x0}}{2} + Y_{F1}\,\frac{1}{\tan\theta} = 0$$

$$X_{F1} = \frac{H_{x0}}{2} - \frac{Y_{F1}}{\tan\theta}$$

$$= \frac{H_{x0}}{2} - \left(\frac{H_{x0}}{2} + \frac{b_x}{4}\right)$$

$$= - \frac{b_x}{4} .$$

From figure 9b

$$\Sigma F_x = 0$$

$$X_{F1} + X_{B1} + 2\left(\frac{b_x}{4d}\right) d + \frac{H_{x0}}{2} = 0$$

$$X_{B1} = - X_{F1} - \frac{b_x}{2} - \frac{H_{x0}}{2}$$

$$= \frac{b_x}{4} - \frac{b_x}{2} - \frac{H_{x0}}{2}$$

$$= - \left(\frac{b_x}{4} + \frac{H_{x0}}{2}\right) .$$

The forces in the x direction at the top of level 2 are identical to the forces at the top of level 1 except for the $b_x/4$ term common to both X_{F1} and X_{B1}. From this it appears that the $H_x/2$ term will be passed on to the back bottom joint of each succeeding level and that the total force of the distributed load will be divided equally between the front and back joints. This hypothesis will be proved using the principal of mathematical induction that states that if a relationship is true for $i = 1$, and if we can prove that when the relationship is true for i, it is also true for $i + 1$, then it is true for all i. In order to begin this proof, the forces in the x direction at the top of level i are assumed to be as shown in figure 9d. The forces in the y direction are given by equations (3) and (4).

From figure 9e,

$$\Sigma M_R = 0$$

$$X_{Fi}\ \frac{d}{2}\ \sin\theta + Y_{Fi}\ \frac{d}{2}\ \cos\theta - Y_{Fi-1}\ \frac{d}{2}\ \cos\theta - \left(\frac{H_{x0}}{2} + \frac{(i-1)b_x}{4}\right)\ \frac{d}{2}\ \sin\theta = 0$$

Substituting equation 3 for Y_{Fi} and Y_{Fi-1}, and eliminating $d/2 \sin\theta$ results in

$$X_{Fi} + \left(\frac{H_{x0}}{2} + \frac{b_x i}{4}\right) i - \left(\frac{H_{x0}}{2} + \frac{b_x(i-1)}{4}\right)(i-1) - \left(\frac{H_{x0}}{2} + \frac{(i-1)\,b_x}{4}\right) = 0$$

$$X_{Fi} + \frac{H_{x0}}{2}(i - (i-1) - 1) + \frac{b_x}{4}(i^2 - (i-1)^2 - (i-1)) = 0$$

$$X_{Fi} + \frac{b_x}{4}(i^2 - (i^2 - 2i + 1) - (i-1)) = 0$$

$$X_{Fi} + \frac{b_x}{4}\ i = 0$$

$$X_{Fi} = \frac{-b_x}{4}\ i\ .$$

From figure 9a

$$\Sigma F_x = 0$$

$$\frac{H_{x0}}{2} + \frac{ib_x}{2} + X_{Bi} + X_{Fi} = 0$$

$$\frac{H_{x0}}{2} + \frac{b_x i}{2} + X_{Bi} - \frac{b_x i}{4} = 0$$

$$X_{Bi} = -\frac{H_{x0}}{2} - \frac{b_x i}{4}\ .$$

This is the desired result. Now equations for X_{Mi} and Y_{Mi} will be derived. Referring to figure 9e,

$$\Sigma F_y = 0$$

$$Y_{Fi\,1} + Y_{Fi} + Y_{Mi} = 0$$

$$\left(\frac{H_{x0}}{2} + \frac{b_x(i-1)}{4}\right)(i-1)\tan\theta + \left(\frac{H_{x0}}{2} + \frac{b_x i}{4}\right) i \tan\theta + Y_{Mi} = 0$$

$$Y_{Mi} = -\left(\frac{H_{x0}}{2}\tan\theta\,(i-1+i)\right) - \left(\frac{b_x}{4}\tan\theta\,((i-1)^2 + i^2)\right)$$

$$= -\left(\frac{H_{x0}\,(2i-1)}{2} + \frac{b_x(2i^2-2i+1)}{4}\right)\tan\theta\,.$$

$$\Sigma F_x = 0$$

$$\left(\frac{H_{x0}}{2} + \frac{(i-1)\,b_x}{4}\right) + X_{Fi} + \frac{b_x}{4d}\,d + X_{Mi} = 0$$

$$\left(\frac{H_{x0}}{2} + \frac{(i-1)\,b_x}{4}\right) - \frac{b_x}{4}\,i + \frac{b_x}{4} + X_{Mi} = 0$$

$$\frac{H_{x0}}{2} + \frac{b_x}{4}(i-1-i+1) + X_{Mi} = 0$$

$$X_{Mi} = -\frac{H_{x0}}{2}$$

In summary,

$$X_{Bi} = -\left(\frac{H_{x0}}{2} + \frac{ib_x}{4}\right),$$

$$X_{Fi} = -\frac{ib_x}{4}\,,$$

$$Y_{Fi} = -\,Y_{Bi} = \left(\frac{H_{x0}}{2} + \frac{ib_x}{4}\right) i \tan\theta\,,$$

$$X_{Mi} = -\frac{H_{x0}}{2}\,,$$

$$Y_{Mi} = -\left(\frac{H_{x0}\,(2i-1)}{2} + \frac{b_x\,(2i^2-2i+1)}{4}\right)\tan\theta\,.$$

Front Joints Pinned

Now the loading condition will be considered with the front joints at the top of the lift pinned. As before, the weight of the lift will be included in the analysis. A freebody diagram of the lift up to level i is shown in figure 10a.

The derivation of Y_{Bi} and Y_{Fi} is exactly the same as the previous case and is therefore omitted. From the insight gained in the previous derivation, it is assumed that $H_{x0}/2$ will be passed on to the front top joint of each succeeding level and that the distributed load will be divided equally between the front and back joints. This assumption will be proved using the principle of mathematical induction as before. The assumed loads are shown in figures 10b. and 10c.

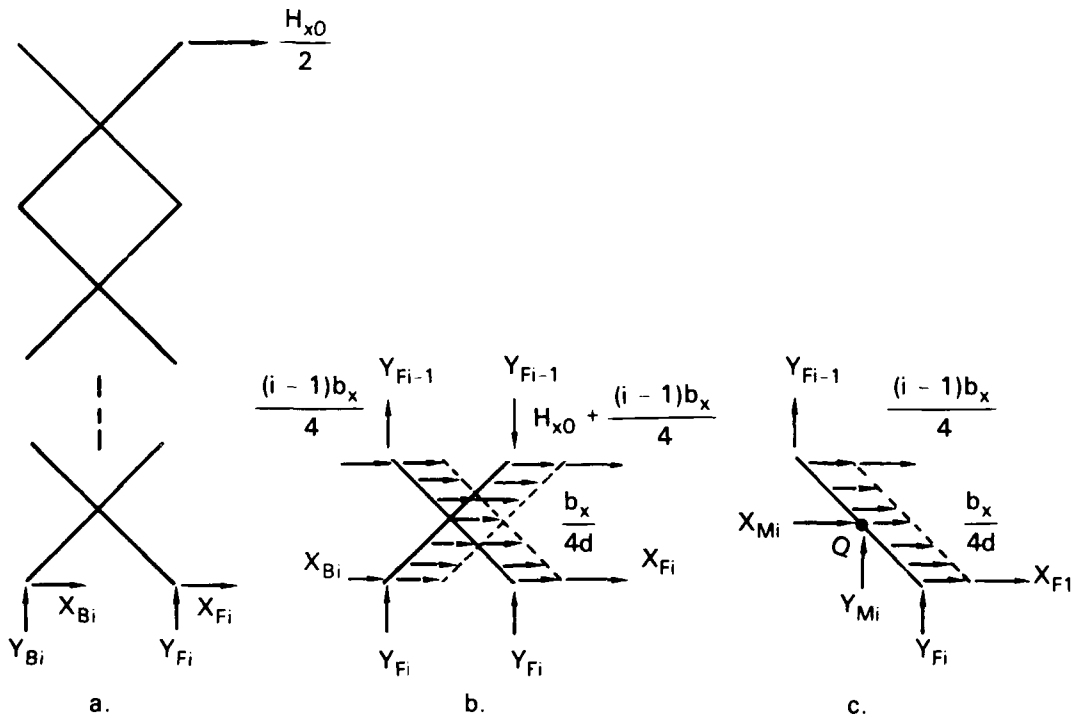

Figure 10. Freebody diagrams for load applied in the x direction with the front joints pinned.

From figure 10c.

$$\Sigma M_Q = 0 ,$$

$$X_{Fi} \frac{d}{2} \sin\theta + Y_{Fi} \frac{d}{2} \cos\theta - Y_{Fi-1} \frac{d}{2} \cos\theta - \frac{(i-1)b_x}{4} \frac{d}{2} \sin\theta = 0 .$$

Substituting equation 3 for Y_{Fi} and $Y_{Fi\,1}$ and eliminating $d/2 \sin\theta$ gives

$$X_{Fi} + \left(\frac{H_{x0}}{2} + \frac{ib_x}{4}\right) i - \left(\frac{H_{x0}}{2} + \frac{(i-1)b_x}{4}\right)(i-1) - \frac{(i-1)b_x}{4} = 0 .$$

$$X_{Fi} = \frac{H_{x0}}{2} (-i + i - 1) + \frac{b_x}{4} (-i^2 + (i-1)^2 + (i-1))$$

$$= -\frac{H_{x0}}{2} + \frac{b_x}{4}(-i^2 + i^2 - 2i + 1 + i - 1)$$

$$= -\left(\frac{H_{x0}}{2} + \frac{b_x i}{4}\right).$$

From figure 10a

$$\Sigma F_x = 0$$

$$\frac{H_{x0}}{2} + X_{Bi} + X_{Fi} + \frac{ib_x}{2} = 0,$$

$$\frac{H_{x0}}{2} + X_{Bi} - \left(\frac{H_{x0}}{2} + \frac{b_x i}{4}\right) + \frac{ib_x}{2} = 0,$$

$$X_{Bi} = -\frac{b_x i}{4}.$$

This is the desired result. The reaction forces at the middle joints will now be found. Referring to figure 10c,

$$\Sigma F_x = 0$$

$$X_{Mi} + \frac{b_x}{4d} d + X_{Fi} + \frac{(i-1)\,b_x}{4} = 0$$

$$X_{Mi} + \frac{b_x}{4} - \left(\frac{H_{x0}}{2} + \frac{b_x i}{4}\right) + \frac{(i-1)\,b_x}{4} = 0$$

$$X_{Mi} = \frac{H_{x0}}{2}.$$

$$\Sigma F_y = 0$$

$$\left(\frac{H_{x0}}{2} + \frac{b_x(i-1)}{4}\right)(i-1)\tan\theta + Y_{Mi} + \left(\frac{H_{x0}}{2} + \frac{b_x i}{4}\right) i \tan\theta = 0$$

$$Y_{Mi} = -\frac{H_{x0}}{2}(i - 1 + i)\tan\theta - \frac{b_x}{4}[(i-1)^2 + i^2]\tan\theta$$

$$= -\left(\frac{H_{x0}(2i-1)}{2} + \frac{b_x\,(2i^2 - 2i + 1)}{4}\right)\tan\theta.$$

In summary,

$$X_{Bi} = -\frac{ib_x}{4},$$

$$X_{Fi} = -\left(\frac{H_{x0}}{2} + \frac{ib_x}{4}\right),$$

$$Y_{Fi} = -Y_{Bi} = \left(\frac{H_{x0}}{2} + \frac{ib_x}{4}\right) i \tan\theta,$$

$$X_{Mi} = \frac{H_{x0}}{2},$$

$$Y_{Mi} = -\left(\frac{H_{x0}(2i-1)}{2} + \frac{b_x(2i^2 - 2i + 1)}{4}\right) \tan\theta.$$

$$Z_i = Z_{Mi} = 0$$

3.1.4 Load 4: Centered Load in the Positive z Direction

This load is once again made more general by including the distributed weight of the lift in the z direction. The z component of the lift weight was previously defined as B_z, and the z component of one level as b_z. Let H_{z0} equal the applied load at the top of the lift, and H_{zi} equal H_{z0} plus the weight of the lift in the z direction up to and including level i. If b_z is the same for every level then

$$H_{zi} = H_{z0} + ib_z,$$

where,

$$b_z = \frac{B_z}{n}.$$

A basic scissor structure with this load is shown in figure 11. This case is more difficult to analyze than the earlier cases because some of the reaction forces depend on the rigidity of the crossbracing between the two sets of scissors (i.e., between the left and right sides). Figure 12 is the front view of the lift and shows the deformations and reaction forces in the y and z directions for lifts with and without crossbracing. The lift with crossbracing is similar to an I-beam and is, of course, the more rigid of the two lifts. In the following analysis the lift with crossbracing will be assumed. Because the load is in the y-z plane and because the scissor is symmetric about the y-z plane the reaction forces are also symmetric about the y-z plane. Mathematically this means that

$$X_{FRi} = -X_{BRi},$$

$$X_{FLi} = -X_{BLi},$$

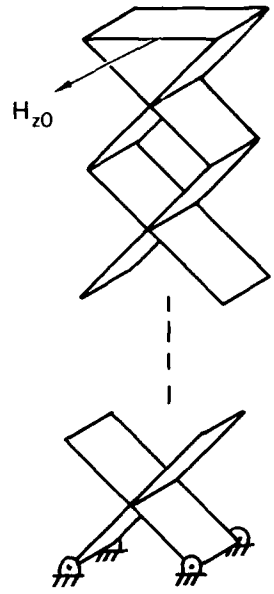

Figure 11. Basic scissor structure with load applied in the positive z direction.

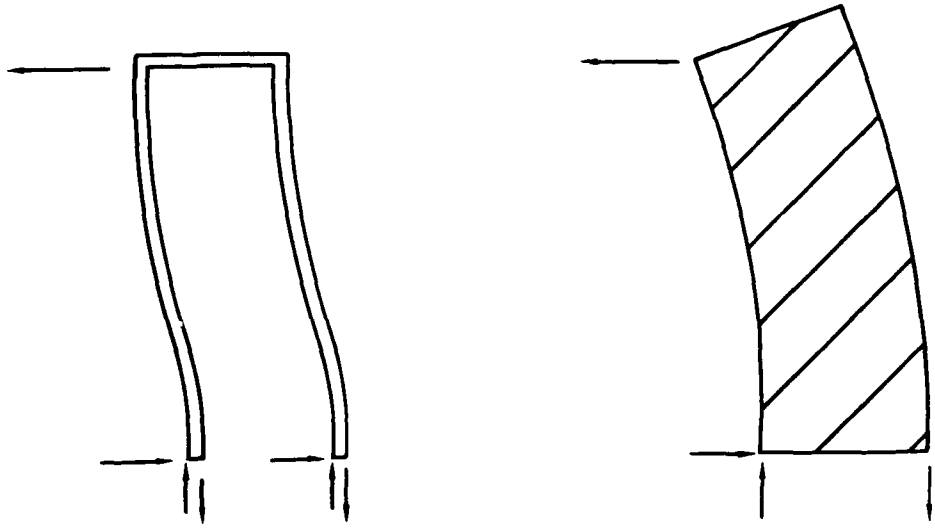

Figure 12. Deflections and reaction forces for load applied in the positive z direction.

$$Y_{FRi} = Y_{BRi} ,$$

$$Y_{FLi} = Y_{BLi} ,$$

$$Y_{MLi} = Y_{MRi} = 0 ,$$

$$Z_{Mi} = 0 ,$$

$$Z_{FRi} = Z_{BRi} ,$$

$$Z_{FLi} = Z_{BLi} .$$

Considering only the front of the lift, the reaction forces in the y direction on the ith level are as shown in figure 13a. The equations for Y_{Ri} and Y_{Li} are derived as follows.

$$\Sigma M_p = 0$$

$$\frac{H_{z0}}{2} id \sin\theta + \left(\frac{ib_z}{2}\right) \frac{id \sin\theta}{2} + Y_{Li} w = 0$$

$$Y_{Li} = -\left(\frac{H_{z0}}{2} + \frac{ib_z}{4}\right) \frac{id \sin\theta}{w} .$$

$$\Sigma F_y = 0$$

$$Y_{Ri} = -Y_{Li} = \left(\frac{H_{z0}}{2} + \frac{ib_z}{4}\right) \frac{id \sin\theta}{w} .$$

The equations for Z_{Ri} and Z_{Li} are found by summing the forces in the z direction.

$$\Sigma F_z = 0 ,$$

$$Z_{Ri} + Z_{Li} + \frac{H_{z0}}{2} + \frac{ib_z}{2} = 0 ,$$

$$Z_{Ri} + Z_{Li} = -\left(\frac{H_{z0} + ib_z}{2}\right) .$$

The individual values of Z_{Ri} and Z_{Li} depend on the tolerances of the lift; however we will assume that they are equal. Letting $Z_{Ri} = Z_{Li} = Z_i$ results in

$$2Z_i = -\left(\frac{H_{z0} + ib_z}{2}\right) ,$$

$$Z_i = -\left(\frac{H_{z0} + ib_z}{4}\right) .$$

Before proceeding with the analysis some comments need to be made. In all of the loads previously analyzed, the reaction forces on the left side were always the same as the

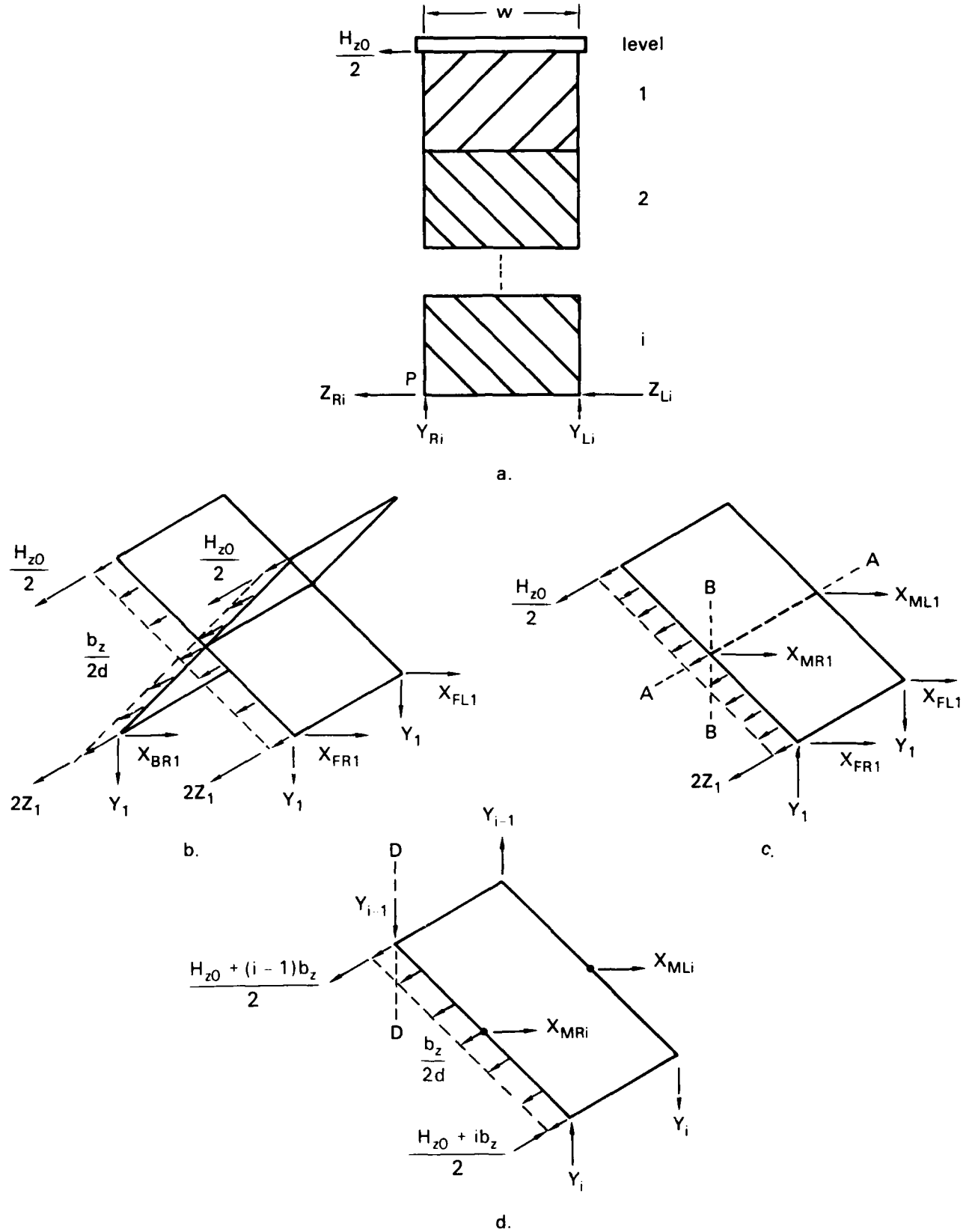

Figure 13. Freebody diagrams for load applied in the positive z direction.

right side. As a result, the crossbracing is completely unstressed allowing the sides of the lift to be analyzed as separate entities. In this case, the loads on the right and left sides are not equal which means that the right and left scissor members can no longer be analyzed separately. The loads on level 1 are shown in figure 13b and 13c. In this figure Z_{R1} and Z_{L1} have been added together and are shown acting on the right side to simplify the drawing. This does not affect the remaining analysis.

Referring to figure 13c

$$\Sigma M_{AA} = 0 ,$$

$$X_{FR1} + X_{FL1} = 0 ,$$

$$X_{FR1} = -X_{FL1} .$$

This means that the net force in the x direction on the front pins must be zero. Although the sum of X_{FRi} and X_{LRi} is zero the individual values are not necessarily zero. Summing moments about BB indicates that there must be a net force in the x direction on the left side of the lift. This net force is the sum of X_{ML1} and X_{FL1}. The actual values of X_{MLi} and X_{FLi} are very difficult to determine because the problem is statically indeterminate. In the following analysis, it will be assumed that the x forces at the bottom joints are equal to zero. This means that

$$X_{FLi} = X_{FRi} = X_{BLi} = X_{BRi} = 0 .$$

This assumption may not be totally valid, but it should be a good approximation as these forces are believed to be small. Figure 13d shows the forces acting on level i.

Now solving for the remaining forces

$$\Sigma F_x = 0$$

$$X_{MRi} + X_{MLi} = 0$$

$$X_{MRi} = - X_{MLi} .$$

$$\Sigma M_{DD} = 0$$

$$\left(\frac{H_{z0} + ib_z}{2}\right) d \cos\theta - d \frac{b_z}{2d} \frac{d \cos\theta}{2} - X_{MLi}\, w = 0$$

$$\left(\frac{H_{z0}}{2} + \frac{ib_z}{2} - \frac{b_z}{4}\right) d \cos - X_{MLi} w = 0$$

$$X_{MLi} = \left(\frac{H_{z0}}{2} + \frac{b_z\,(2i - 1)}{4}\right) \frac{d \cos\theta}{w} .$$

In summary,

$$X_i = 0$$

$$Y_{Ri} = -\,Y_{Li} = \frac{H_{z0}}{2} + \frac{ib_z}{4} \quad \frac{id \sin\theta}{w} ,$$

$$Z_i = -\,\frac{H_{z0} + ib_z}{4} ,$$

$$Z_{Mi} = 0 ,$$

$$X_{MLi} = -\,X_{MRi} = \frac{H_{z0}}{2} + \frac{b_z\,(2i - 1)}{4} \quad \frac{d \cos\theta}{w} ,$$

$$Y_{Mi} = 0 .$$

3.1.5 Load 5: Moment About the x Axis

This loading condition is shown in figure 14. Again symmetry exists about the y-z plane. Mathematically this means that

$$X_{BRi} = -X_{FRi} ,$$

$$Y_{BRi} = Y_{FRi} ,$$

$$X_{BLi} = -X_{FLi} ,$$

$$Y_{BLi} = Y_{FLi} ,$$

$$Y_{MLi} = Y_{MRi} = 0 .$$

Also, since the applied load has no Z component, all the reaction loads in the Z direction are zero, i.e.,

$$Z_{Mi} = Z_i = 0 .$$

The front half of the lift is shown in figure 15a. From this figure,

$$\Sigma M_p = 0 ,$$

$$Y_{Ri}\, w - \frac{M_x}{2} = 0 ,$$

$$Y_{Ri} = \frac{M_x}{2w} .$$

$$\Sigma F_y = 0 ,$$

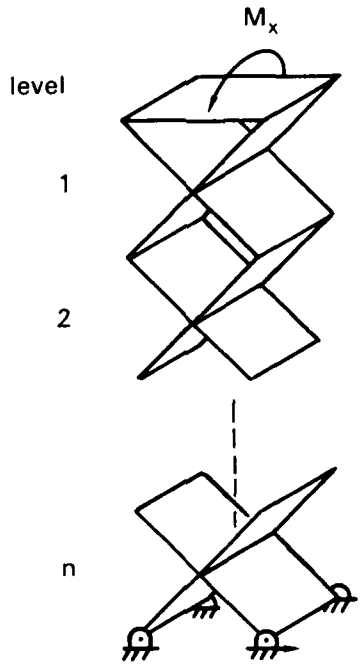

Figure 14. Basic scissor structure with applied moment about the x axis.

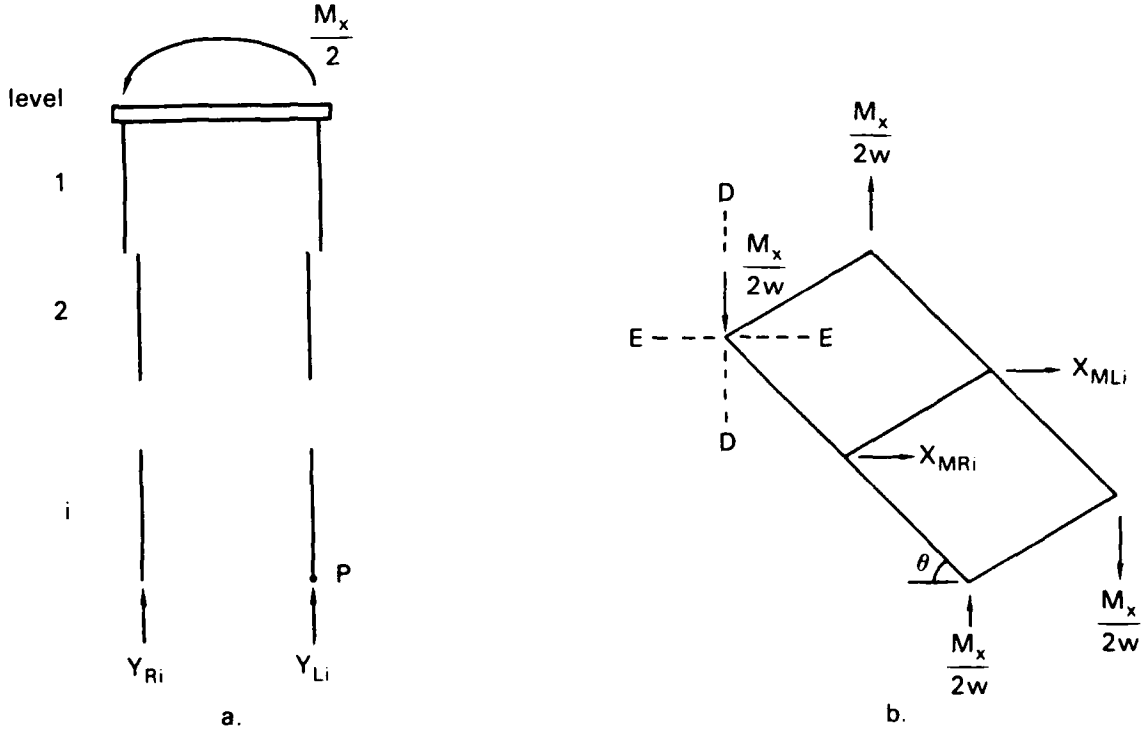

Figure 15. Freebody diagrams for an applied moment about the x axis.

$$Y_{Ri} + Y_{Li} = 0 ,$$

$$Y_{Li} = - \frac{M_x}{2w} .$$

This shows that the y forces are independent of the scissor level. As with the previous load, we assume that the x forces at the ends of the members are zero. The remaining reaction loads are shown in figure 15b. Summing the moments about DD and summing the forces in the x direction gives

$$X_{MLi} = X_{MRi} = 0 .$$

In summary,

$$X_i = 0 ,$$

$$Y_{Ri} = -Y_{Li} = \frac{M_x}{2w} ,$$

$$X_{Mi} = 0 ,$$

$$Y_{Mi} = 0 .$$

$$Z_{Mi} = Z_i = 0$$

3.1.6 Load 6: Moment About the y Axis

A moment load about the z axis is shown in figure 16. In order to simplify the analysis, several assumptions will be made. First, all joints, including the top ones, are assumed to be pinned. Second, the y forces at the bottom of each level are assumed to be zero. Because the applied load at the top of the lift has no y component, the summation of the y forces at the bottom of each level must be zero. This does not require that the individual forces be zero; even so, the assumption will be made. Third, the reaction forces in the x z plane are assumed to act in the direction shown in figure 17a.

The above assumptions are necessary because the problem is statically indeterminate. If information about the deflection of the joints was available, then the problem might possibly be analyzed more accurately. However, this information is not available. The reaction forces at the bottom of level i are now determined from figure 17a and 17b.

$$\alpha = \tan^{-1} \frac{w}{d \cos \theta} .$$

$$\Sigma M_p = 0$$

$$M_y - 4R_i \frac{(d^2 \cos^2 \theta + w^2)^{1/2}}{2} = 0$$

$$R_i = \frac{M_y}{2(d^2 \cos^2 \theta + w^2)^{1/2}} .$$

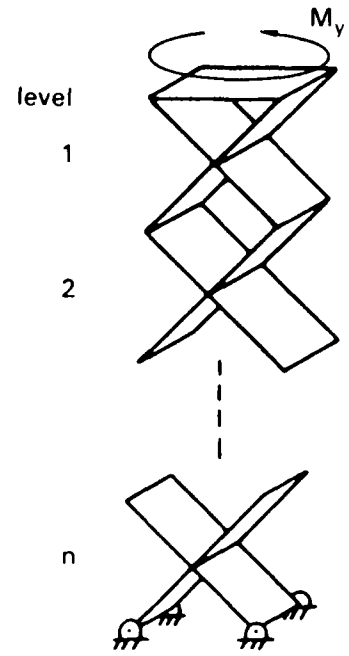

Figure 16. Basic scissor structure with applied moment about the y axis.

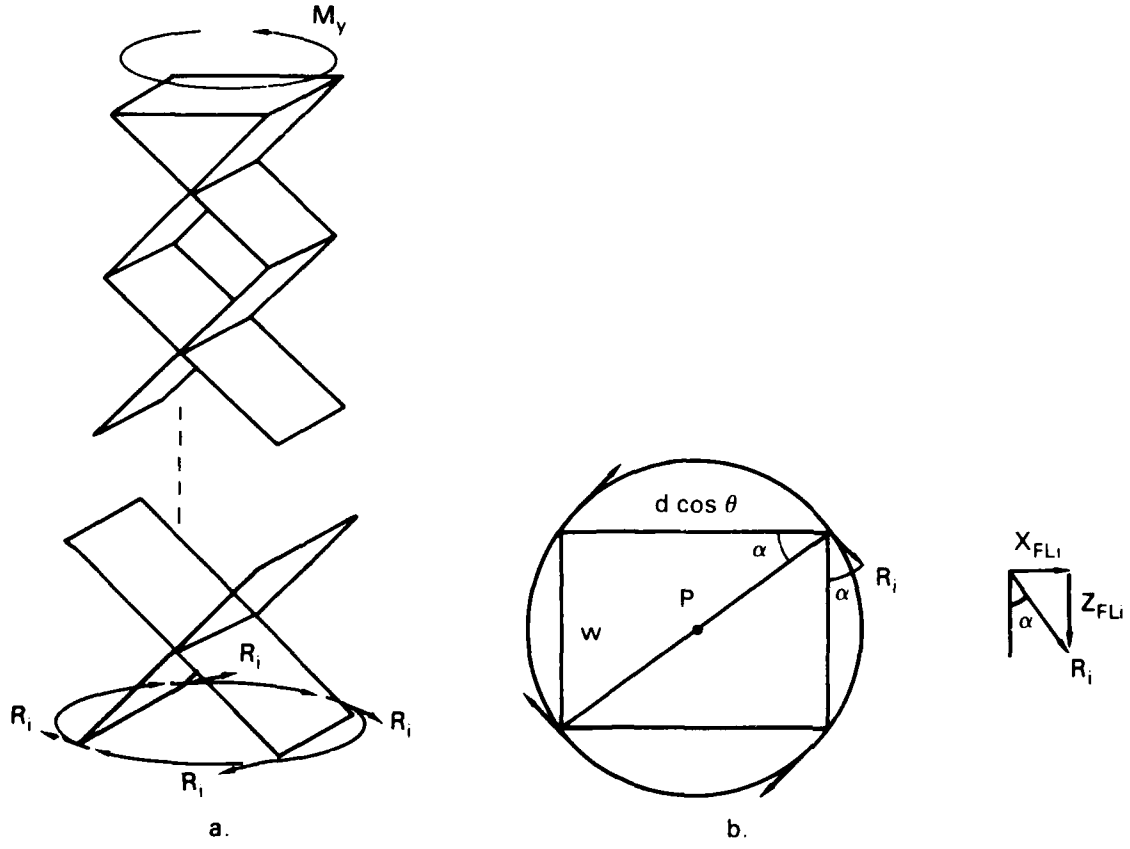

Figure 17. Freebody diagrams for an applied moment about the y axis.

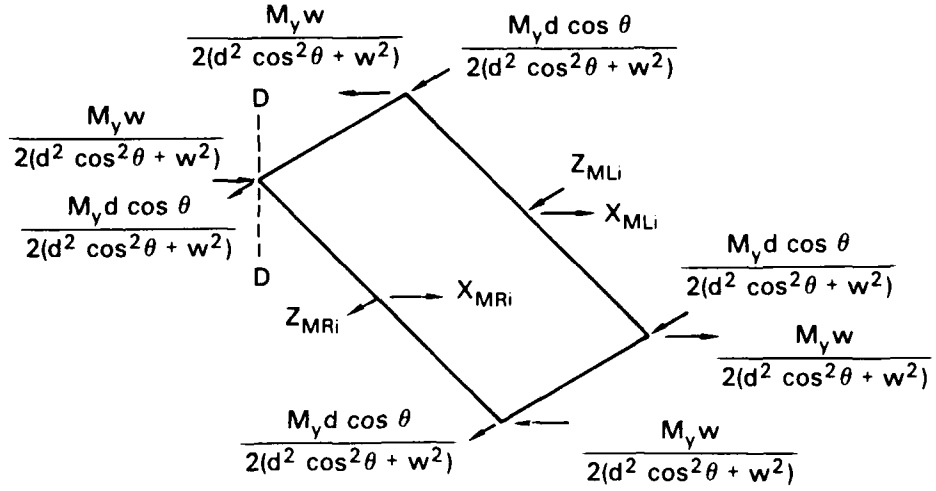

c.

Figure 17. Freebody diagrams for an applied moment about the y axis (continued).

$$X_{FLi} = R_i \sin\alpha ,$$

$$= \frac{M_y \sin\alpha}{2(d^2 \cos^2\theta + w^2)^{1/2}} ,$$

but $$\sin\alpha = \frac{w}{(d^2 \cos^2\theta + w^2)^{1/2}} ,$$

$$X_{FLi} = \frac{M_y w}{2(d^2 \cos^2\theta + w^2)} ,$$

$$Z_{FLi} = R_i \cos\alpha$$

$$= \frac{M_y \cos\alpha}{2(d^2 \cos^2\theta + w^2)^{1/2}} ,$$

but $$\cos\alpha = \frac{d \cos\theta}{(d^2 \cos^2\theta + w^2)^{1/2}} ,$$

$$Z_{FLi} = \frac{M_y d \cos\theta}{2(d^2 \cos^2\theta + w^2)} .$$

The remaining analyses will be completed by referring to figure 17c. The magnitudes of Z_{MLi} and Z_{MRi} depend on the tolerances of the lift. If one of the middle joints makes contact before the other middle joint, then that joint could possible carry the entire load, and after summing the forces in the z direction Z_{MLi} and Z_{MRi} are given by

$$Z_{MLi} \text{ or } Z_{MRi} = \frac{2M_y d \cos\theta}{d^2 \cos^2\theta + w^2} ,$$

with the other one equal to zero.

However, if they share the load equally, then

$$Z_{MLi} = Z_{MRi} = Z_{Mi}$$

$$= - \frac{M_y d \cos \theta}{(d^2 \cos^2 \theta + w^2)} .$$

In this analysis Z_{MLi} and Z_{MRi} are assumed to be equal. Equations for X_{MLi} and X_{MRi} are calculated as follows.

$$\Sigma M_{DD} = 0$$

$$X_{MLi} = 0.$$

$$\Sigma F_x = 0$$

$$X_{MLi} + X_{MRi} = 0$$

$$X_{MRi} = 0.$$

In summary,

$$X_{FLi} = X_{BLi} = \frac{M_y w}{2(d^2 \cos^2 \theta + w^2)}$$

$$X_{FRi} = X_{BRi} = \frac{-M_y w}{2(d^2 \cos^2 \theta + w^2)}$$

$$Z_{FLi} = Z_{FRi} = \frac{M_y d \cos \theta}{2(d^2 \cos^2 \theta + w^2)}$$

$$Z_{BLi} = Z_{BRi} = \frac{-M_y d \cos \theta}{2(d^2 \cos^2 \theta + w^2)}$$

$$Z_{MLi} = Z_{MRi} = \frac{M_y d \cos \theta}{(d^2 \cos^2 \theta + w^2)}$$

$$Y_i = Y_{Mi} = 0 .$$

$$X_{Mi} = 0$$

It is emphasized that the equations for this load should be used with some reservation because of the original assumptions. The equations should give a reasonable approximation, but should not be taken as exact.

3.2 EQUATIONS FOR THE ACTUATOR

There are at least two methods of calculating the actuator forces required to raise the scissor lift. The first method is to use equations of static equilibrium. In this method, the general equations derived in the previous section are used to determine the reaction forces that are not affected by the actuators. Equations of static equilibrium are then used to solve for the remaining forces including the actuator force. The problem with this method is that for most actuator placements a set of at least five simultaneous equations results. This method is, therefore, not recommended.

The second method is to use the principle of conservation of energy. In this method friction forces are assumed to be zero, requiring that work in equals work out. This assumption makes it possible to calculate the actuator forces directly, simplifying the analysis of the scissor levels containing the actuator. The equations in this section are derived using this principle.

Referring to figure 1, it is noted that of the six possible loads, only H_x and H_y result in work as the lift elevates, and H_x contributes only if it is applied to the joints that move in the x direction. All other loads have no tendency to raise or lower the lift, therefore making no contribution.

Figure 18 shows a 4-level lift with loads applied in the x and y directions. Notice that the distributed weight of the lift is accounted for by B_y and B_x acting at the center of the lift. The validity of this model is proven as follows. Consider the uniform mass shown in figure 19. The total potential energy stored in the mass is given by

$$E = \lim_{\Delta m_i \to 0} \Sigma g \Delta m_i \, y_i$$

where g = acceleration due to gravity.

$$E = \lim_{\Delta y_i \to 0} \Sigma g(\rho u w \Delta y_i) \, y_i$$

$$= \int_0^h \rho g u w y \, dy \, .$$

If the weight is evenly distributed, then $\rho g u w = \frac{W}{h}$, and

$$E = \frac{W}{h} \int_0^h y \, dy \, .$$

$$= \frac{W}{h} \frac{y^2}{2} \Big|_0^h \, .$$

$$= \frac{Wh}{2} \, .$$

Now if the block height increases but the total weight stays the same, then

$$\text{Work} = E_2 \quad E_1$$

$$= \frac{W(h_2 \quad h_1)}{2} \, .$$

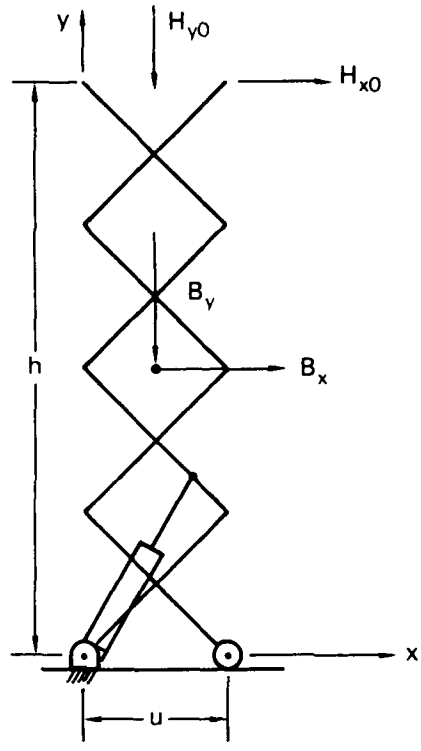

Figure 18. Four level lift loaded in the x and y directions.

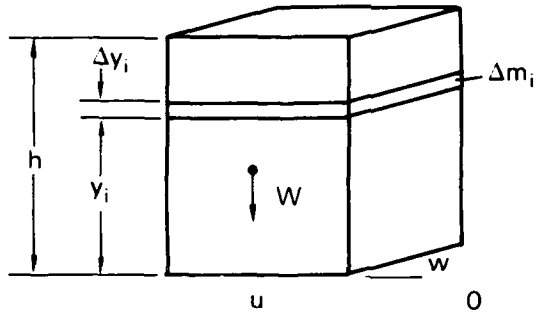

Figure 19. Uniform mass.

Applying the principle of the conservation of energy gives

$$-\left(H_{y0}+\frac{B_y}{2}\right)(h-h_0)+\left(H_{xo}+\frac{B_x}{2}\right)(u-u_0)+\int_{\ell_0}^{\ell} F\,dr=0 \qquad (5)$$

where F = force exerted by the actuator

ℓ = length of the actuator

r = dummy variable.

Taking the derivative with respect to ℓ gives

$$-\left(H_{y0}+\frac{B_y}{2}\right)\frac{dh}{d\ell}+\left(H_{x0}+\frac{B_x}{2}\right)\frac{du}{d\ell}+F=0$$

But $du/d\ell$ can be expressed in terms of $dh/d\ell$ as follows.

$$h=n(d^2-u^2)^{1/2},$$

$$\frac{dh}{d\ell}=\frac{1}{2}\,n(d^2-u^2)^{1/2}(-2u)\,\frac{du}{d\ell},$$

$$=\frac{-nu}{(d^2-u^2)^{1/2}}\,\frac{du}{d\ell},$$

$$=\frac{-n}{\tan\theta}\,\frac{du}{d\ell},$$

$$\frac{du}{d\ell}=-\frac{\tan\theta}{n}\,\frac{dh}{d\ell}.$$

Making the appropriate substitution gives

$$-\left[\left(H_{y0}+\frac{B_y}{2}\right)+\left(H_{x0}+\frac{B_x}{2}\right)\frac{\tan\theta}{n}\right]\frac{dh}{d\ell}+F=0,$$

$$F=K\,\frac{dh}{d\ell},$$

where $K=\left(H_{y0}+\frac{B_y}{2}\right)+\left(H_{x0}+\frac{B_x}{2}\right)\frac{\tan\theta}{n}$.

In order to use this equation, an expression of h as a function of ℓ must be derived. The derivative of the expression is then taken to give $dh/d\ell$. These functions are designated by $f(\ell)$ and $g(\ell)$ as shown below.

$$h = f(\ell) ,$$

$$\frac{dh}{d\ell} = g(\ell) .$$

As an example of this method, the actuator forces on an n-level lift with two actuators attached to the bottom of the lift will be analyzed. The right side of the lift is shown in figure 20. The lift is assumed to be on a horizontal surface so that the weight of the lift has only the y component, B_y. The only load that is applied at the top of the lift is H_{y0}. The formulas for $f(\ell)$ and $g(\ell)$ are derived as follows.

$$h = n \sqrt{d^2 - \ell^2} ,$$

$$\frac{dh}{d\ell} = n \frac{1}{2} (d^2 - \ell^2)^{-1/2}(-2\ell) ,$$

$$= \frac{-n\ell}{(d^2 - \ell^2)^{1/2}} .$$

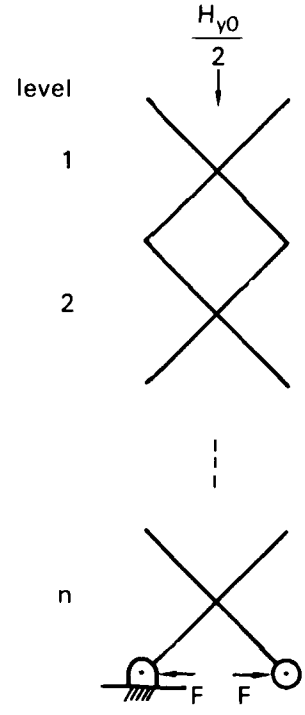

Figure 20. n-level lift with actuators attached between the bottom joints.

The last equation can be expressed in terms of θ by noting that,

$$\frac{\ell}{(d^2 - \ell^2)^{1/2}} = \frac{1}{\tan \theta} ,$$

$$\frac{dh}{d\ell} = \frac{-n}{\tan\theta} .$$

Substituting this equation into equation 5 gives

$$F = -\frac{1}{2}\left(H_{y0} + \frac{B_y}{2}\right)\frac{n}{\tan\theta} ,$$

$$= -\frac{1}{2}\left(H_{y0} + \frac{nb_y}{2}\right)\frac{n}{\tan\theta} .$$

As expected, this formula is identical to the formula for X_{Bi} in load 1 in section 3.1 except that i is replaced by n.

For many actuator locations, the derivation of $f(\ell)$ and $g(\ell)$ is quite straightforward. For other locations, the derivation is more difficult. General formulas can be derived for calculating $g(\ell)$. Two sets of formulae will be derived. The first set assumes that both ends of the actuator are attached to points on the lift. The second set of equations assumes that only one end of the actuator is attached to the lift with the other end attached to a fixed point. This second set of equations can also be used to calculate the force of an actuator with both ends attached to the lift; however, the first set of equations is easier to use.

Some common equations are used in both derivations. These equations are presented below. Consider the n-level lift shown in figure 21. As shown, the back joints at the bottom of the lift are pinned to a fixed point, and the origin of the x-y axis has been shifted to correspond with this point. The coordinates of a point Q on a positive sloping member is given by

$$x_Q = \text{ad} \cos\theta , \tag{6}$$

$$y_Q = (n - i + a)\, d \sin\theta , \tag{7}$$

where $0 \leq a \leq 1$

For a point Q on a negatively sloping member, the formula for y_Q remains the same; however, the equation for x_Q becomes

$$x_Q = (1 - a)d \cos\theta . \tag{8}$$

An interesting observation is now made. If the equations for x_Q and y_Q are squared, then for positive sloping members

$$x_Q^2 = a^2 d^2 \cos^2\theta ,$$

$$y_Q^2 = (n - i + a)^2\, d^2 \sin^2\theta ,$$

$$\cos^2\theta = \frac{x_Q^2}{a^2 d^2} ,$$

$$\sin^2\theta = \frac{y_Q^2}{(n - i + a)^2 d^2} .$$

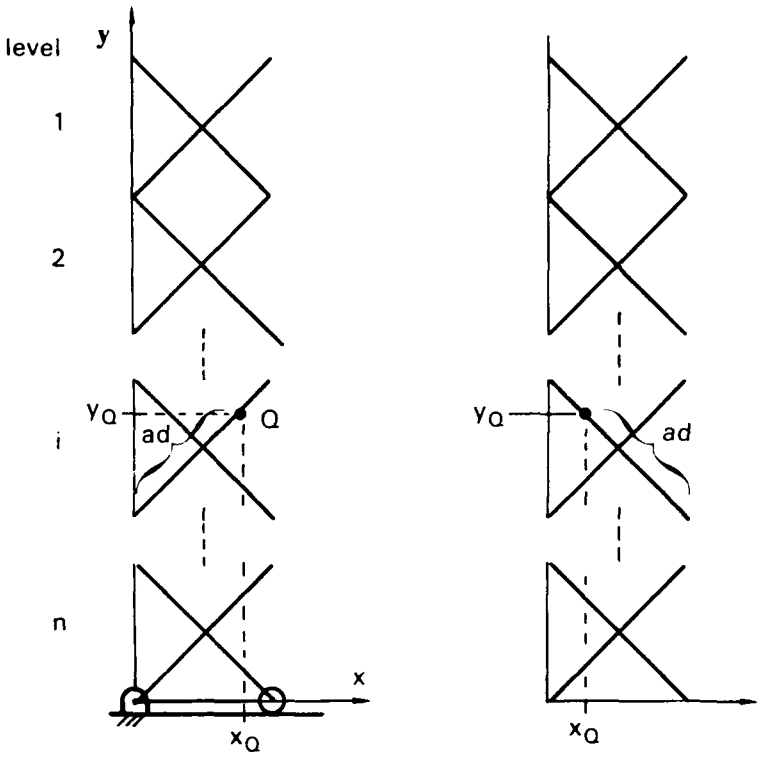

Figure 21. Coordinates of a point on the lift.

Adding the previous two equations gives

$$1 = \frac{x_Q^2}{a^2 d^2} + \frac{y_Q^2}{(n - i + a)^2 d^2} .$$

This is the equation of the ellipse shown in figure 22. This ellipse is the path traveled by point Q. If the point is on a negatively sloping member, the x-axis intercepts are $\pm(1 - a)d$. If a force is being applied to point Q to raise the lift, maximum mechanical advantage will occur when the force is tangent to this path.

3.2.1 Derivation of $dh/d\ell$ Assuming Both Actuator Ends are Pinned to a Scissor Member:

Before beginning the derivation, observe that because both ends of the actuator are pinned to scissor members, the actuator (and all of the scissor members) will lie along the x axis when $\theta = 0°$ and along the y axis when $0 = 90°$. Let

ℓ_0 = length of the actuator for $\theta = 0°$

ℓ_{90} = length of the actuator for $\theta = 90°$.

Assume that the actuator is attached to points P and Q on the lift. Equations (6), (7), and (8) can be made more general by letting x_{P0} and x_{Q0} equal the x coordinate of points P and Q respectively for $\theta = 0$, and y_{P90} and y_{Q90} equal the y coordinates of the points for $\theta = 90°$. From figure 21, it is observed that

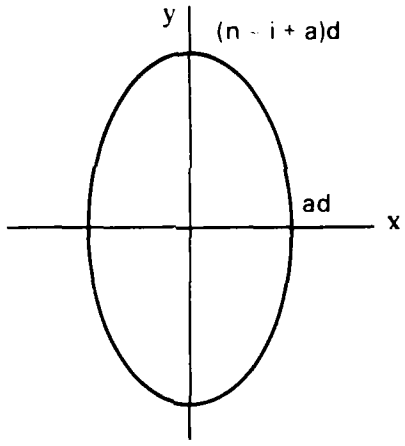

Figure 22. Path traveled by a point on a positively sloping scissor member.

$$x_{Q0} = \begin{cases} a_Q d \text{ for positively sloping members,} \\ (1 - a_Q)d \text{ for negatively sloping members,} \end{cases}$$

$$x_{P0} = \begin{cases} a_P d \text{ for positively sloping members,} \\ (1 - a_P)d \text{ for negatively sloping members,} \end{cases}$$

$$y_{Q90} = (n - i_Q + a_Q)d ,$$

$$y_{P90} = (n - i_P + a_P)d .$$

The equations for x_Q, y_Q, x_P, and y_P become

$$x_Q = x_{Q0} \cos \theta ,$$

$$y_Q = y_{Q90} \sin \theta ,$$

$$x_P = x_{P0} \cos \theta ,$$

$$y_P = y_{P90} \sin \theta .$$

If the x and y components of the actuator length are designated by ℓ_x and ℓ_y respectively, then

$$\ell_x = \left| x_Q - x_P \right| ,$$

$$= \left| (x_{Q0} - x_{P0}) \cos \theta \right| ,$$

$$\ell_y = \left| y_Q - y_P \right| ,$$

$$= \left| (y_{Q0} - y_{P0}) \sin \theta \right| .$$

Squaring ℓ_x and ℓ_y gives

$$\ell_x^2 = (x_{Q0} - x_{P0})^2 \cos^2 \theta ,$$

$$= \ell_0^2 \cos^2 \theta ,$$

$$\ell_y^2 = (y_{Q0} - y_{P0})^2 \sin^2 \theta ,$$

$$= \ell_{90}^2 \sin^2 \theta .$$

Solving for $\cos^2 \theta$ and $\sin^2 \theta$ gives

$$\cos^2 \theta = \frac{\ell_x^2}{\ell_0^2} ,$$

$$\sin^2 \theta = \frac{\ell_y^2}{\ell_{90}^2} .$$

Adding $\cos^2 \theta$ and $\sin^2 \theta$ results in

$$1 = \frac{\ell_x^2}{\ell_0^2} + \frac{\ell_y^2}{\ell_{90}^2} .$$

This is the equation of the ellipse shown in figure 23. The length of the actuator is given by

$$\ell^2 = \ell_x^2 + \ell_y^2 ,$$

$$= \ell_0^2 \cos^2 \theta + \ell_{90}^2 \sin^2 \theta ,$$

$$= \ell_0^2 (1 - \sin^2 \theta) + \ell_{90}^2 \sin^2 \theta ,$$

$$= (\ell_{90}^2 - \ell_0^2) \sin^2 \theta + \ell_0^2 . \qquad (9)$$

But

$$\sin \theta = \frac{h}{nd} . \qquad (10)$$

Therefore

$$\ell^2 = (\ell_{90}^2 - \ell_0^2) \frac{h^2}{n^2 d^2} + \ell_0^2 ,$$

$$h^2 = \frac{(\ell^2 - \ell_0^2) n^2 d^2}{(\ell_{90}^2 - \ell_0^2)} . \qquad (11)$$

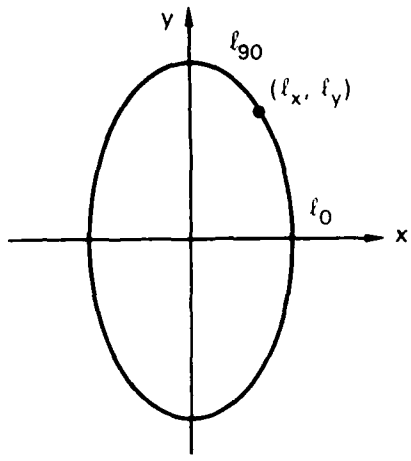

Figure 23. Length of an actuator attached between two points on a lift.

Taking the derivative of h with respect to ℓ results in

$$2h \frac{dh}{d\ell} = \frac{2\ell n^2 d^2}{(\ell_{90}^2 - \ell_0^2)} ,$$

$$\frac{dh}{d\ell} = \frac{\ell n^2 d^2}{(\ell_{90}^2 - \ell_0^2)h} .$$

h can be replaced with the square root of equation 11 giving

$$\frac{dh}{d\ell} = \frac{\ell n^2 d^2}{(\ell_{90}^2 - \ell_0^2)} \left(\frac{\ell_{90}^2 - \ell_0^2}{(\ell^2 - \ell_0^2) n^2 d^2} \right)^{1/2} .$$

$$\boxed{\frac{dh}{d\ell} = \frac{\ell nd}{(\ell_{90}^2 - \ell_0^2)} \left(\frac{\ell_{90}^2 - \ell_0^2}{\ell^2 - \ell_0^2} \right)^{1/2} .}$$

This equation can be expressed in terms of θ by replacing ℓ with the equality given in equation (9). This results in

$$\frac{dh}{d\ell} = \frac{nd[(\ell_{90}^2 - \ell_0^2) \sin^2 \theta + \ell_0^2]^{1/2}}{(\ell_{90}^2 - \ell_0^2)} \left(\frac{\ell_{90}^2 - \ell_0^2}{[(\ell_{90}^2 - \ell_0^2) \sin^2 \theta + \ell_0^2] - \ell_0^2} \right)^{1/2}$$

$$= \frac{nd(\ell_{90}^2 \sin^2 \theta + \ell_0^2 \cos^2 \theta)^{1/2}}{(\ell_{90}^2 - \ell_0^2)} \left(\frac{\ell_{90}^2 - \ell_0^2}{(\ell_{90}^2 - \ell_0^2) \sin^2 \theta} \right)^{1/2}$$

$$= \frac{nd(\ell_{90}^2 \sin^2 \theta + \ell_0^2 \cos^2 \theta)^{1/2}}{(\ell_{90}^2 - \ell_0^2) (\sin^2 \theta)^{1/2}} ,$$

$$\frac{dh}{d\ell} = \frac{nd\left(\ell_{90}^2 + \frac{\ell_0^2}{\tan^2\theta}\right)^{1/2}}{(\ell_{90}^2 - \ell_0^2)} .$$

The equation can also be written in terms of h by replacing $\sin\theta$ with equation (10). The result is

$$\frac{dh}{d\ell} = \frac{n^2 d^2}{(\ell_{90}^2 - \ell_0^2)} \left[\frac{(\ell_{90}^2 - \ell_0^2)}{n^2 d^2} + \left(\frac{\ell_0}{h}\right)^2\right]^{1/2} .$$

3.2.2 Derivation of $dh/d\ell$ Assuming One Actuator End is Pinned to Ground.

It is possible to derive an equation relating h to ℓ for an actuator with one end pinned to a fixed point using the techniques of the section 3.2.1; however, the resulting equations are extremely complicated. In this section, the equation for $dh/d\ell$ will be derived as a function of the angle of the scissor members from the x axis, the angle of the actuator from the x axis, and the point of load application. Figure 24 shows an n-level lift with a force applied at point Q. In figure 24, $\bar{s}$ is the unit vector tangent to the path traversed by point Q (see figure 22). The equations for x_Q and y_Q were previously found to be

$$x_Q = x_{Q0} \cos\theta ,$$

$$y_Q = y_{Q90} \sin\theta . \qquad (12)$$

Taking the derivation with respect to θ gives

$$\frac{dx_Q}{d\theta} = -x_{Q0} \sin\theta ,$$

$$\frac{dy_Q}{d\theta} = y_{Q90} \cos\theta ,$$

$$\frac{dy_Q}{dx_Q} = \frac{\left(\frac{dy_Q}{d\theta}\right)}{\left(\frac{dx_Q}{d\theta}\right)} ,$$

$$= \frac{y_{Q90} \cos\theta}{-x_{Q0} \sin\theta} ,$$

$$= \frac{-y_{Q90}}{x_{Q0} \tan\theta} .$$

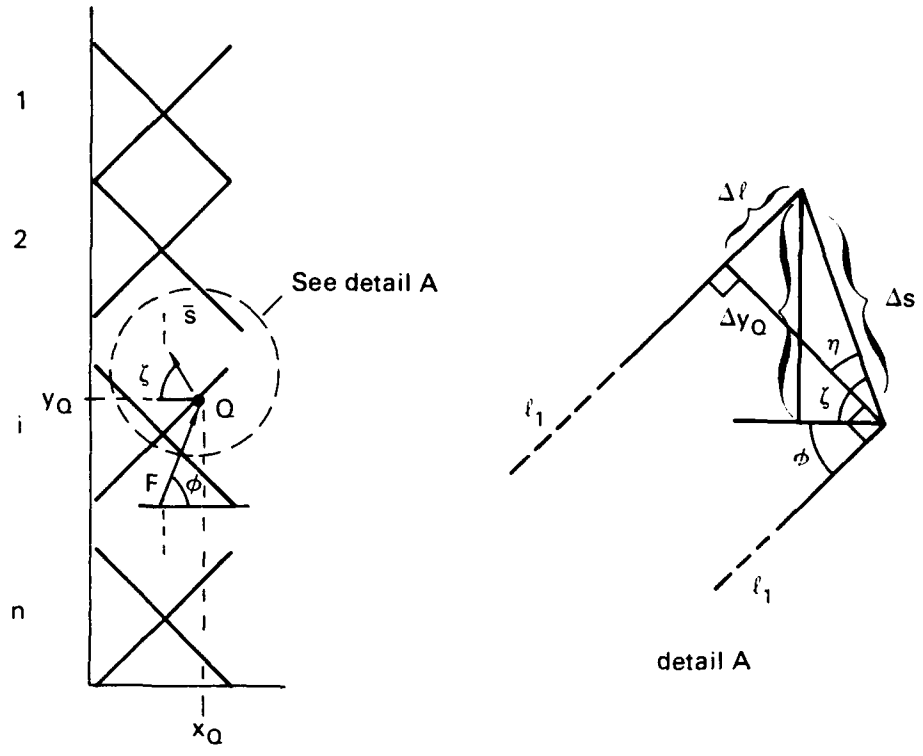

Figure 24. Actuator position and displacement nomenclature.

This is the slope of $\bar{s}$. ζ is given by

$$\zeta = \tan^{-1} \frac{y_{Q90}}{x_{Q0} \tan \theta} \quad . \tag{13}$$

A small displacement of the actuator is shown in detail A of figure 24.

From figure 24 it is apparent that

$$\frac{dy_Q}{ds} = \lim_{\Delta s \to 0} \frac{\Delta y_Q}{\Delta s} .$$

$$= \sin \zeta , \tag{14}$$

$$\frac{ds}{d\ell} = \lim_{\Delta s \to 0} \frac{\Delta s}{\Delta \ell} .$$

$$= \frac{1}{\sin \eta} ,$$

$$= \frac{-1}{\cos (\eta + 90)}$$

$$= \frac{-1}{\cos (\phi + \zeta)} . \tag{15}$$

The height of the lift in terms of y_Q is given combining equations (10) and (12). The result is

$$h = nd \frac{y_Q}{y_{Q90}} .$$

nd equals the max height of the platform. If the maximum height is designated by h_{max} then

$$h = \frac{h_{max}\, y_Q}{y_{Q90}} ,$$

$$\frac{dh}{dy_Q} = \frac{h_{max}}{y_{Q90}} . \tag{16}$$

The derivative of h with respect to ℓ is found from equations (14), (15), and (16).

$$\frac{dh}{d\ell} = \frac{dh}{dy_Q} \frac{dy_Q}{ds} \frac{ds}{d\ell} ,$$

$$= \frac{h_{max}}{y_{Q90}} \left(\frac{\sin \zeta}{\cos (\phi + \zeta)} \right) .$$

If the other end of the actuator is attached to a fixed point P then ϕ can be determined from the following formula.

$$\phi = \tan^{-1} \frac{y_Q - y_P}{x_Q - x_P} .$$

In summary, for positively sloping members

$$x_{Q0} = \begin{cases} a_Q d \text{ for positively sloping members} \\ (1 - a_Q)d \text{ for negatively sloping members} \end{cases}$$

$$y_{Q90} = (n - i_Q + a_Q)d$$

$$x_Q = x_{Q0} \cos\theta$$

$$y_Q = y_{Q90} \sin\theta$$

$$\phi = \tan^{-1}\left(\frac{y_Q - y_P}{x_Q - x_P}\right)$$

$$\zeta = \tan^{-1}\frac{y_{Q90}}{x_{Q0}\tan\theta}$$

$$\frac{dh}{d\ell} = \frac{h_{\max}}{y_{Q90}}\left(\frac{-\sin\zeta}{\cos(\zeta + \phi)}\right).$$

Before proceeding, a word of caution needs to be made about the formula for determining ϕ. ϕ can be any angle from 0° to 360°. Care must be taken to select the proper angle since calculators always give angles from −90° to +90°. Because ζ is always between 0 and 90°, ζ does not have this ambiguity.

These formulas can also be used to determine $dh/d\ell$ for an actuator with both ends attached to points on the lift. This is done by modeling the actuator as two actuators, each having one end pinned to ground.

An actuator attached to two points on a lift and pushing with force F is shown in figure 25a. In order to analyze this problem, the single actuator is replaced with two actuators each pushing with force F as shown in figures 25b and 25c. Notice that one end of each of these actuators is attached to a fixed point. Assuming that friction is negligible requires that

$$W_{in} = W_{out}.$$

Modifiying equation 5 of section 3.2 to account for the two actuators results in

$$\left(H_{x0} + \frac{B_x}{2}\right)(h - h_0) + \left(H_{x0} + \frac{B_x}{2}\right)(u - u_0) + \int_{\ell_0}^{\ell_1} F dr_1 + \int_{\ell_0}^{\ell_2} F dr_2 = 0.$$

But $h = n(d^2 - u^2)^{1/2}$.

$$u = \left(d^2 - \frac{h^2}{n^2}\right)^{1/2}.$$

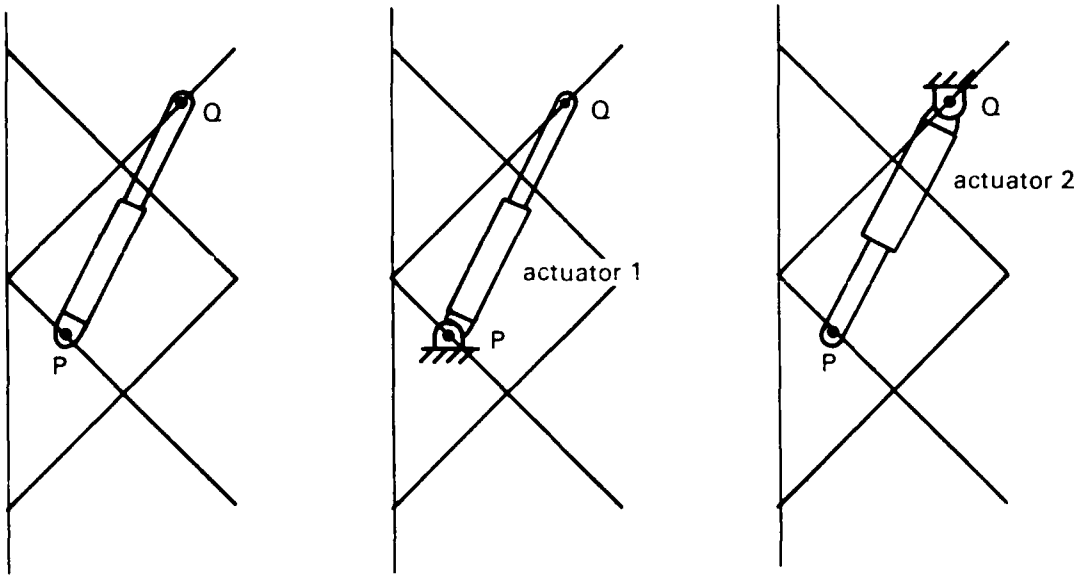

Figure 25. Actuator models.

Substituting the above equation for u gives

$$-\left(H_{y0}+\frac{B_y}{2}\right)(h-h_0)+\left(H_{x0}+\frac{B_x}{2}\right)\left[\left(d^2-\frac{h^2}{n^2}\right)^{1/2}-\left(d^2-\frac{h_0^2}{n^2}\right)^{1/2}\right]+\int_{\ell_0}^{\ell_1} F dr_1+\int_{\ell_0}^{\ell_2} F dr_2=0 .$$

Taking the derivative with respect to h gives

$$-\left(H_{y0}+\frac{B_y}{2}\right)+\left(H_{x0}+\frac{B_x}{2}\right)\frac{1}{2}\left(d^2-\frac{h^2}{n^2}\right)^{1/2}\left(-\frac{2h}{n^2}\right)+F\frac{d\ell_1}{dh}+F\frac{d\ell_2}{dh}=0 ,$$

$$-\left(H_{y0}+\frac{B_y}{2}\right)-\left(H_{x0}+\frac{B_x}{2}\right)\frac{\left(\frac{h}{n}\right)}{n\left(d^2-\frac{h^2}{n^2}\right)^{1/2}}+F\left(\frac{d\ell_1}{dh}+\frac{d\ell_2}{dh}\right)=0 .$$

But $\dfrac{\frac{h}{n}}{\left(d^2-\frac{h^2}{n^2}\right)^{1/2}}=\tan\theta$.

Therefore,

$$-\left(H_{y0} + \frac{B_y}{2}\right) - \left(H_{x0} + \frac{B_x}{2}\right) \frac{\tan\theta}{n} + F\left(\frac{d\ell_1}{dh} + \frac{d\ell_2}{dh}\right) = 0 .$$

$$F = K \frac{1}{\frac{d\ell_1}{dh} + \frac{d\ell_2}{dh}} .$$

$$= K\left(\frac{1}{\frac{1}{\left(\frac{dh}{d\ell_1}\right)} + \frac{1}{\left(\frac{dh}{d\ell_2}\right)}}\right),$$

where $K = \left(H_{y0} + \frac{B_y}{2}\right) + \left(H_{x0} + \frac{B_x}{2}\right) \frac{\tan\theta}{n}$.

The term in the large parenthesis is equal to $dh/d\ell$. Now, use the previous equations to find $dh/d\ell_1$ and $dh/d\ell_2$.

4.0 CALCULATION OF REACTION FORCES

A scissor lift with a single actuator in levels i and i + 1 is shown in figure 26a. As mentioned in section 3.0, the scissor members above level i and below level i + 1 can be modelled as two basic scissor structures. The model for members i thru i - 1 is not shown because the analysis and interpretation of the forces in this model are straightforward. A possible model for members i + 2 thru n is shown in figure 26b. This model was obtained by rotating the members 180 degrees about the z axis. The joints at the top of level i + 2 are identified by the letters a, b, c, and d. The corresponding joints in the model are similarly identified. In order to determine the applied loads at the top of this model, the reaction forces at the bottom of the lift are first determined by performing a freebody analysis on the entire lift. These loads are then applied to the top of the model by reversing the x and y forces and moments (including the x and y components of the weight of the lift) while leaving the z forces and moments the same. Now the reaction forces throughout the model are determined using the equations of section 3.1. The weight of the model is negative in these calculations. The forces at the bottom of level i + 1 are obtained by transfering the loads at joints a, b, c, and d at the bottom of the model to the corresponding joint at the bottom of level i + 1. When transfering the loads, the x and y forces are transfered directly but the z forces must be reversed. The reaction forces in level 1 to i - 1 are calculated using the equations from section 3.1. The loads at the top of level i are obtained by reversing all of the reaction forces at the bottom of level i - 1. The actuator force is now found using the equations of section 3.2. Finally, the reactions forces in levels i and i + 1 are found using equations of static equilibrium.

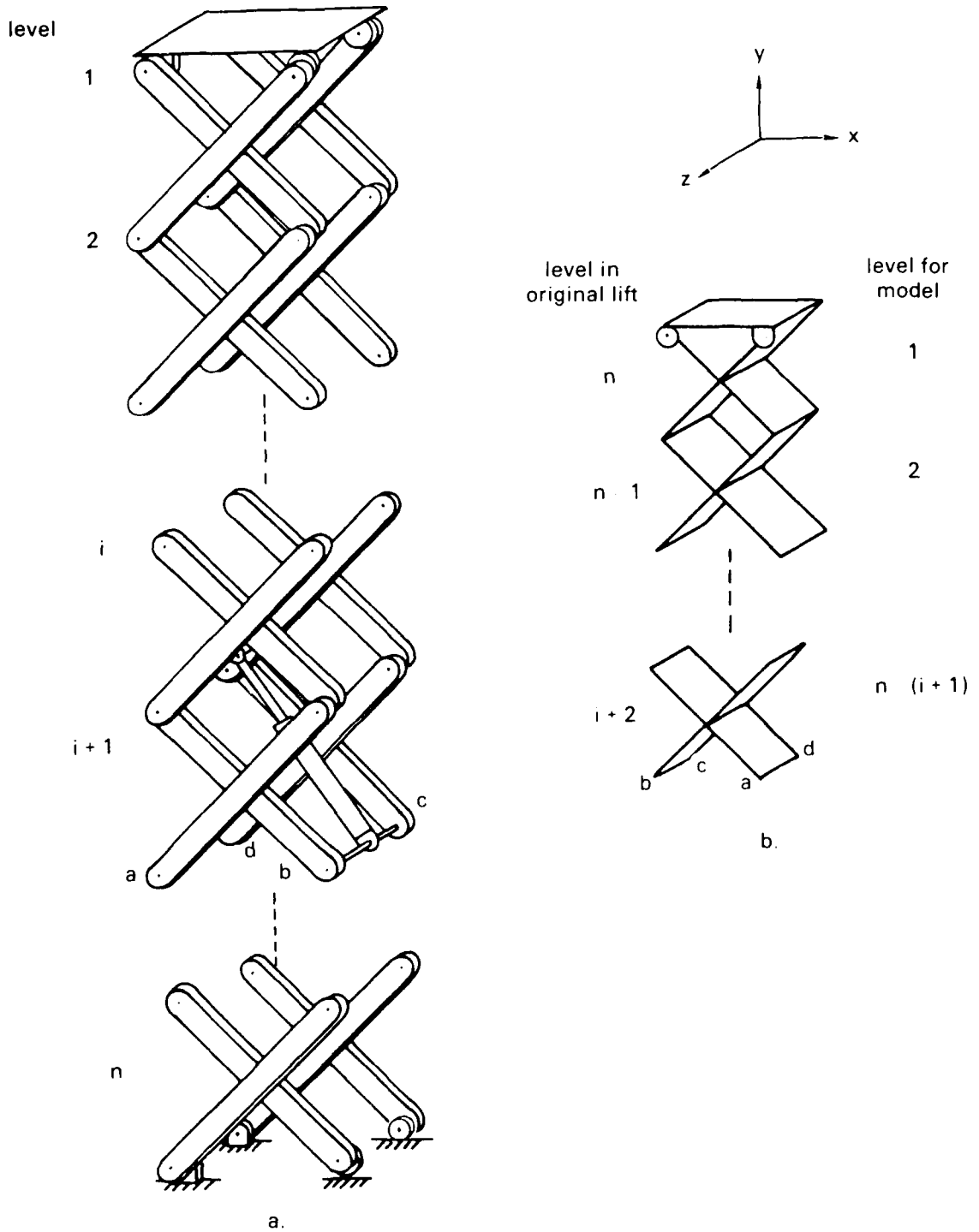

Figure 26. Detailed n-level scissor lift.

5.0 ACTUATOR PLACEMENT

With the results of the previous section, several design issues can now be discussed. The first is actuator placement. Several actuator constraints must be considered when selecting a location. These constraints include the minimum retracted length, maximum extended length, and maximum available force. Constraints imposed by the lift include strength of scissor members and space constraints imposed by the lift (and possibly by the payload). Proper actuator placement can significantly reduce the maximum force required of the actuator and also reduce the reaction forces at the lift joints. This in turn allows the designer to use cheaper and lighter parts in the design.

Figure 27 shows several possible locations for a single actuator on a three-level lift. Equations for $dh/d\ell$ in terms of θ were determined and are given in table 1. Figure 28 plots these equations for $5° \leq \theta \leq 90°$. Of the five positions, position 3 results in the lowest actuator force for small values of θ. The problem with this position is that the distance between the two joints goes to zero as the lift height approaches zero allowing no storage space for the actuator. If there is vacant space beneath the lift and if the actuator is properly designed, then this position can still be used.

An interesting subtlety is illustrated by positions 2 and 5. Position 5 was purposely selected to coincide with position 2 at $\theta = 10°$. Even though the points coincide at this angle, using the fixed point results in a force that is nearly half that of the moving point-a significant reduction. The disadvantage of position 5, is that the final extended length is much larger than that of position 2.

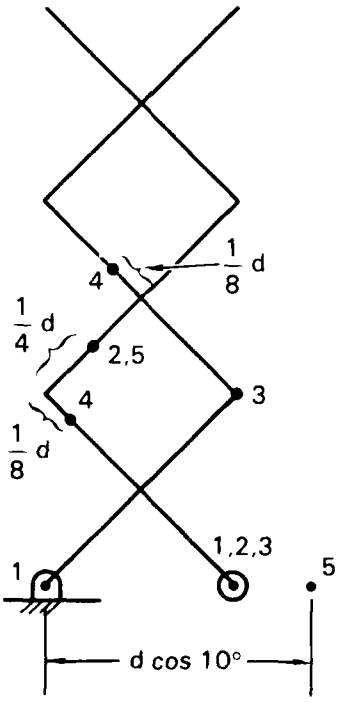

Figure 27. Possible actuator locations.

Table 1. Comparison of $dh/d\ell$ for several actuator locations.

Actuator Position	Equation for $dh/d\ell$	$dh/d\ell$ for $\theta = 10°$	$dh/d\ell$ for $\theta = 5°$
1	$\frac{-3}{\tan\theta}$	-17.0	-34.3
2	$\frac{3}{4}\left(25 + 9\,\frac{1}{\tan^2\theta}\right)^{1/2}$	13.3	26.0
3	3	3	3
4	$\frac{3}{2}\left(9 + \frac{1}{\tan^2\theta}\right)^{1/2}$	9.62	17.7
5	$\frac{-12\sin\zeta}{5\cos(\zeta+\phi)}$ where $\phi = \tan^{-1}\frac{\frac{5}{4}\sin\theta}{\frac{1}{4}\cos\theta - \cos 10°}$ $\zeta = \tan^{-1}\frac{5}{\tan\theta}$	7.59	14.69

The actuator force is unaffected by the level in which the actuator is placed; however, the maximum stress in the members (assuming a given cross-section and material) is affected. To illustrate this, consider the weightless lift shown in figure 29a. Only the right side is shown in this figure. In this lift, the actuator (not shown) is assumed to be attached to the lift at points P and Q. Level i is therefore constrained by the actuator, and levels 1 through i - 1 and levels i + 1 through n can be modelled by two basic scissor structures. By applying the appropriate equations from load 1 of section 3.1, the reaction forces at the top and bottom of level i can be calculated and are shown in figure 29b.

In order to determine the stresses in the members, the forces at the joints need to be resolved into normal and tangential loads. The resulting normal and tangential loads are shown in figure 29c. The equations for these forces are derived below.

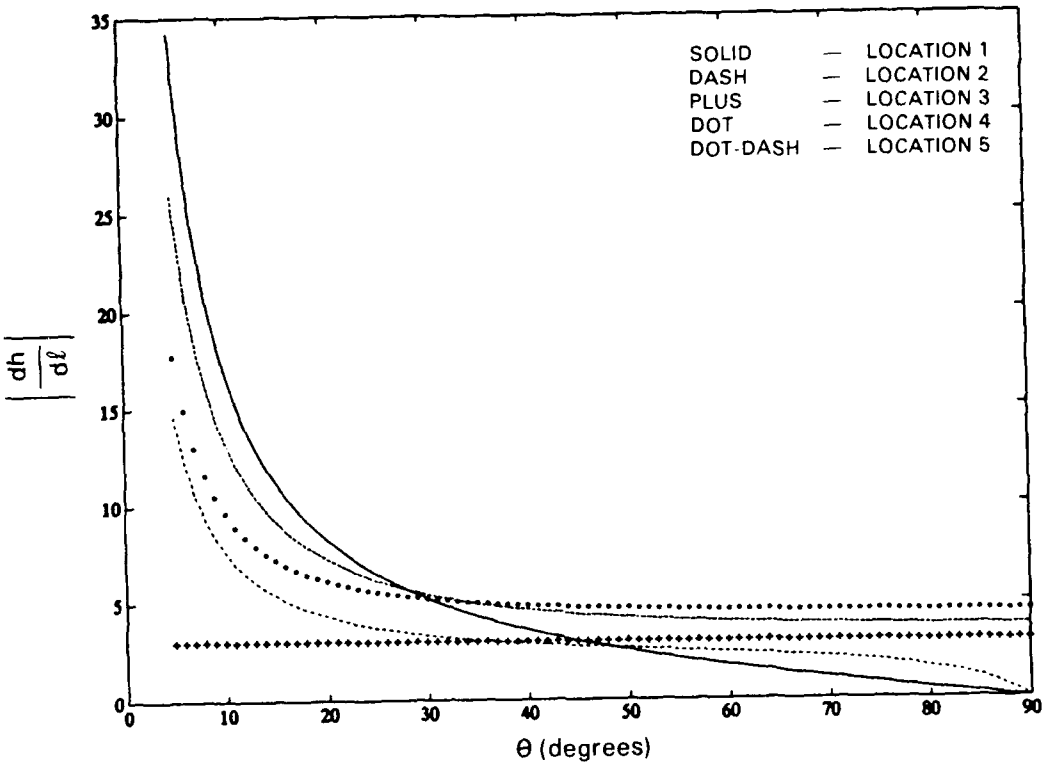

Figure 28. $\left|\frac{dh}{d\ell}\right|$ vs θ.

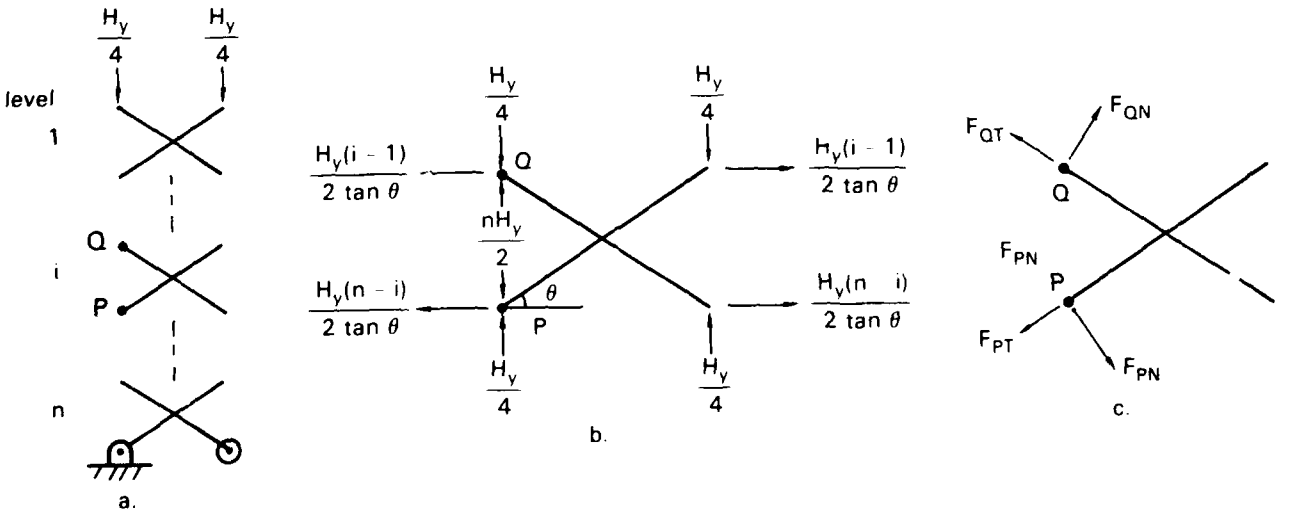

Figure 29. Weightless n-level lift with actuator between left joints of level i.

$$F_{PN} = \frac{nH_y}{2} \cos\theta - \frac{H_y(n-i)}{2\tan\theta} \sin\theta - \frac{H_y}{4} \cos\theta ,$$

$$\frac{F_{PN}}{H_y \cos\theta} = \frac{n}{2} - \frac{n-i}{2} - \frac{1}{4} ,$$

$$= \frac{1}{2} i - \frac{1}{4} . \tag{17}$$

$$F_{QN} = \frac{nH_y}{2} \cos\theta - \frac{H_y(i-1)}{2\tan\theta} \sin\theta - \frac{H_y}{4} \cos\theta$$

$$\frac{F_{QN}}{H_y \cos\theta} = \frac{n}{2} - \frac{i-1}{2} - \frac{1}{4}$$

$$\frac{F_{QN}}{H_y \cos\theta} = -\frac{1}{2} i + \left(\frac{n}{2} + \frac{1}{4}\right) . \tag{18}$$

$$F_{PT} = \frac{nH_y}{2} \sin\theta + \frac{H_y(n-i)}{2\tan\theta} \cos\theta - \frac{H_y}{4} \sin\theta$$

$$\frac{F_{PT}}{H_y \sin\theta} = \frac{n}{2} + \frac{n-i}{2\tan^2\theta} - \frac{1}{4}$$

$$= \frac{-1}{2\tan^2\theta} i + \left(\frac{n}{2} - \frac{1}{4} + \frac{n}{2\tan^2\theta}\right)$$

$$= -\frac{1}{2\tan^2\theta} i + \left(\frac{n}{2\tan^2\theta} + \frac{2n-1}{4}\right) . \tag{19}$$

$$F_{QT} = \frac{nH_y}{2} \sin\theta + \frac{H_y(i-1)}{2\tan\theta} \cos\theta - \frac{H_y}{4} \sin\theta$$

$$\frac{F_{QT}}{H_y \sin\theta} = \frac{n}{2} + \frac{i-1}{2\tan^2\theta} - \frac{1}{4}$$

$$= \frac{1}{2\tan^2\theta} i + \left(\frac{-1}{2\tan^2\theta} + \frac{2n-1}{4}\right) . \tag{20}$$

Equations (17) and (18) are plotted in figure 30a for $n = 7$. Equations (19) and (20) are plotted in figure 30b for $n = 7$ and $\theta = 45°$. From these figures it is seen that in order to reduce the maximum load on any member, the actuator should be placed in the center level of the lift. Adding the weight of the platform will probably shift the ideal level downward.

Although the above analysis was done for a specific actuator orientation, the principle is applicable to any orientation, and the maximum forces can be reduced by placing the actuator in the center of the lift.

Additional mechanical advantage can be achieved by taking advantage of the physical geometries of the scissor members. This is done by mounting the ends of the actuator at the upper or lower sides of the scissor members to improve the angle of attack. When deriving the actuator force equations in section 3.2, it was assumed that the actuator is attached to points on the longitudinal axis of the scissor members. If the end of the actuator is offset from this axis to take advantage of the physical geometries of the scissor members, then the equations no longer apply. Because this technique can reduce the actuator forces significantly, some effort was made to derive equations for this more general case; however, the equations became overly complex. In order to analyze the actuator forces for this case it is recommended that the equations for the basic scissor structure be used to calculate the forces at the top and bottom of the levels containing the actuator, and that the remaining forces (including the actuator force) be calculated using the equations of static equilibrium. Because the actuator force is unknown a set of simultaneous equations will result which can be solved using matrix operations.

In an earlier example, a lift with two parallel actuators attached to the bottom of the lift was assumed. A scissor lift was recently built that used two electric actuators in parallel to raise the lift, although the actuator placement was different from the previous example. It was found that because the actuator motors operated at different speeds the actuators "fought" each other even though they were both driving the lift in the same direction. This resulted in excessive loading of the actuators and nearly caused the motors to stall. Eventually the actuators were replaced with a single, centered actuator to eliminate the problem. Parallel actuation is feasible, but some means of synchronization will likely be necessary. It is unclear whether the problem would have occurred with hydraulic actuators.

One last observation is that the actuator forces are, in general, several times larger than the applied load. If position 5 is used, the reaction forces in the y direction at the bottom sliding joints are negative. This means that these joints must also be constrained in the upward direction, otherwise the lift will tip over.

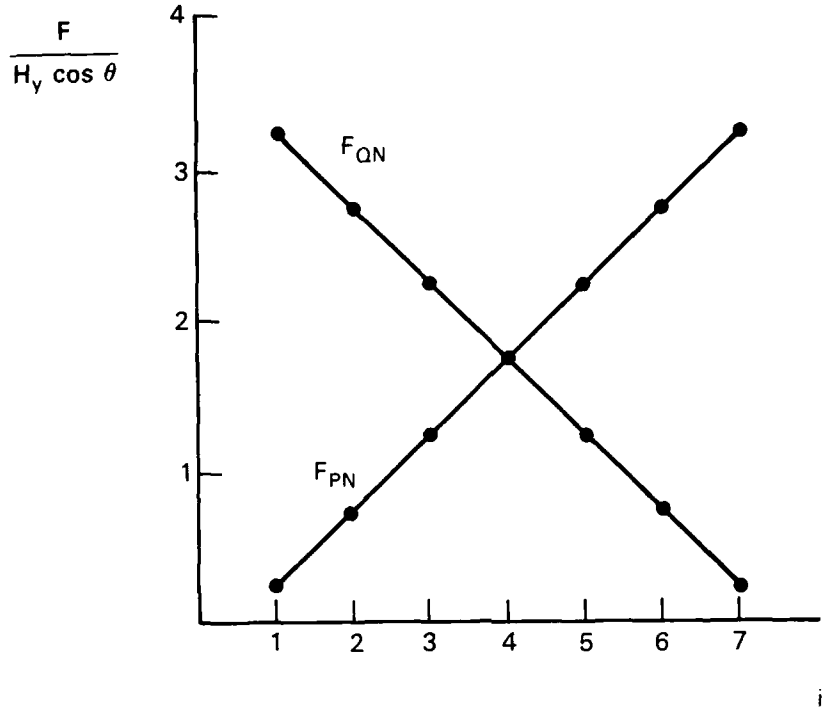

a.

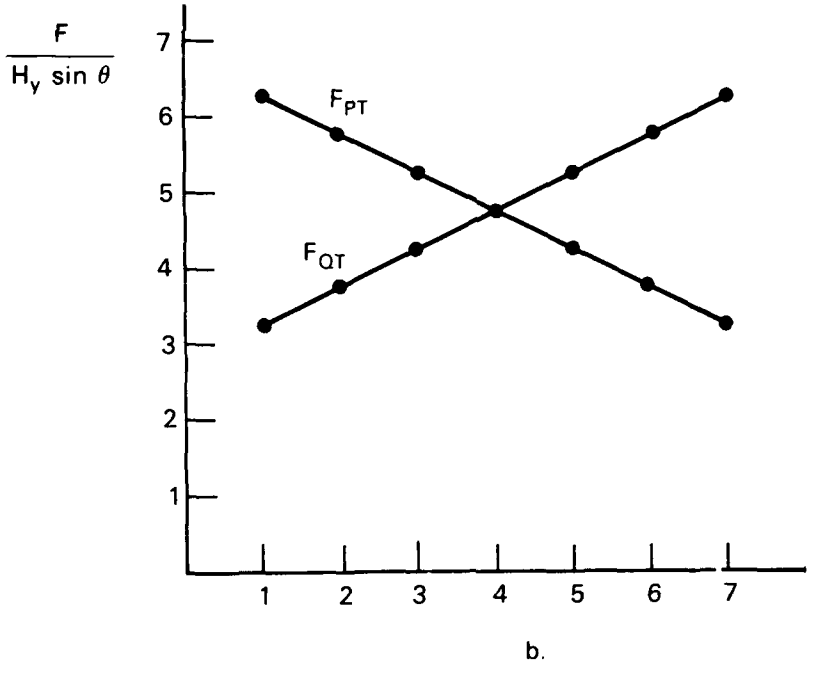

b.

Figure 30. Normal and tangential forces.

6.0 STRENGTH AND RIGIDITY

The reaction loads on the positive sloping members of an arbitrary level of a lift are shown in figure 31. Notice that the reaction forces for loads 1, 2, and 3 are all in the x and y directions. Furthermore, they are symmetrical about the x-y plane. Because of this any crossbracing between the left and right sides of the lift for these loads is completely unstressed. Crossbracing may be used for buckling purposes, but if used these members will not be heavily loaded. Loads 4, 5, and 6 introduce reaction forces that do stress the cross-brace members. In these cases, crossbracing between the sides of the lift is essential for both strength and rigidity. In most applications, the scissor lift operates on level ground. In this application load 1 is the most significant load although loads 2 and 5 may also be present if the load at the top of the lift is not centered. If the lift operates on sloping surfaces, then loads 3, 4, and 6 will also be present. The specific application for which the scissor lift is being designed will, of course, determine the type and amount of crossbracing required.

As previously mentioned, loads 1 through 3 do not stress the crossbraces. As long as θ is not too small (greater than 5°) the most significant component of the reaction loads is the normal component. This component is shown in figure 32a. For these loads it is critical that dimension t be large in order to carry the load efficiently. Rectangular tubing is ideal for this application. Channel beams or I-beams would also be effective.

When loads 4 and 5 are present and θ is small, the loads affecting the crossbracing are the ones shown in figure 32b. In this case dimension t_2 of the crossbaces and dimension t_1 of the scissor members needs to be large in order to carry the load efficiently. Rectangular tubing is ideal in this loading condition because it has a high moment of inertia-to-weight ratio. Channel or I-beam cross sections could also be used. As θ approaches 90° crossbracing becomes less significant because the forces begin to align with the axis of the members.

Load 4 introduces a condition not present in any of the other loads. This condition is shown in figure 32c. A critical dimension in this case is w. Rectangular tubing is again ideal. Channel and I-beam cross sections are less desirable. Crossbracing similar to figure 32d would also be effective for this load.

Load 6 generates the normal forces shown in figure 32b except that for this load, the normal forces are neglible for small values of θ but become larger as θ approaches 90°. Load 6 also generates the condition shown figure 32e. The crossbracing shown in figure 32d is ideal for this condition.

In addition to proper member cross section selection, several other things can be done to make the lift more rigid. One of the assumptions made in calculating the x forces at the ends of the members for loads 4 and 5 was that the ends are not constrained in the x direction. It was admitted that this assumption is not entirely valid especially if the sliding/rollings joints at the top and bottom of the lift are restrained after the lift is deployed. This can be done by using some type of brake, or by using parallel actuators (if actuators are employed at the top and/or bottom of the lift). Removing this degree of freedom will help make the lift more rigid. The other thing that will improve rigidity is keeping the tolerances in the lift as small as possible.

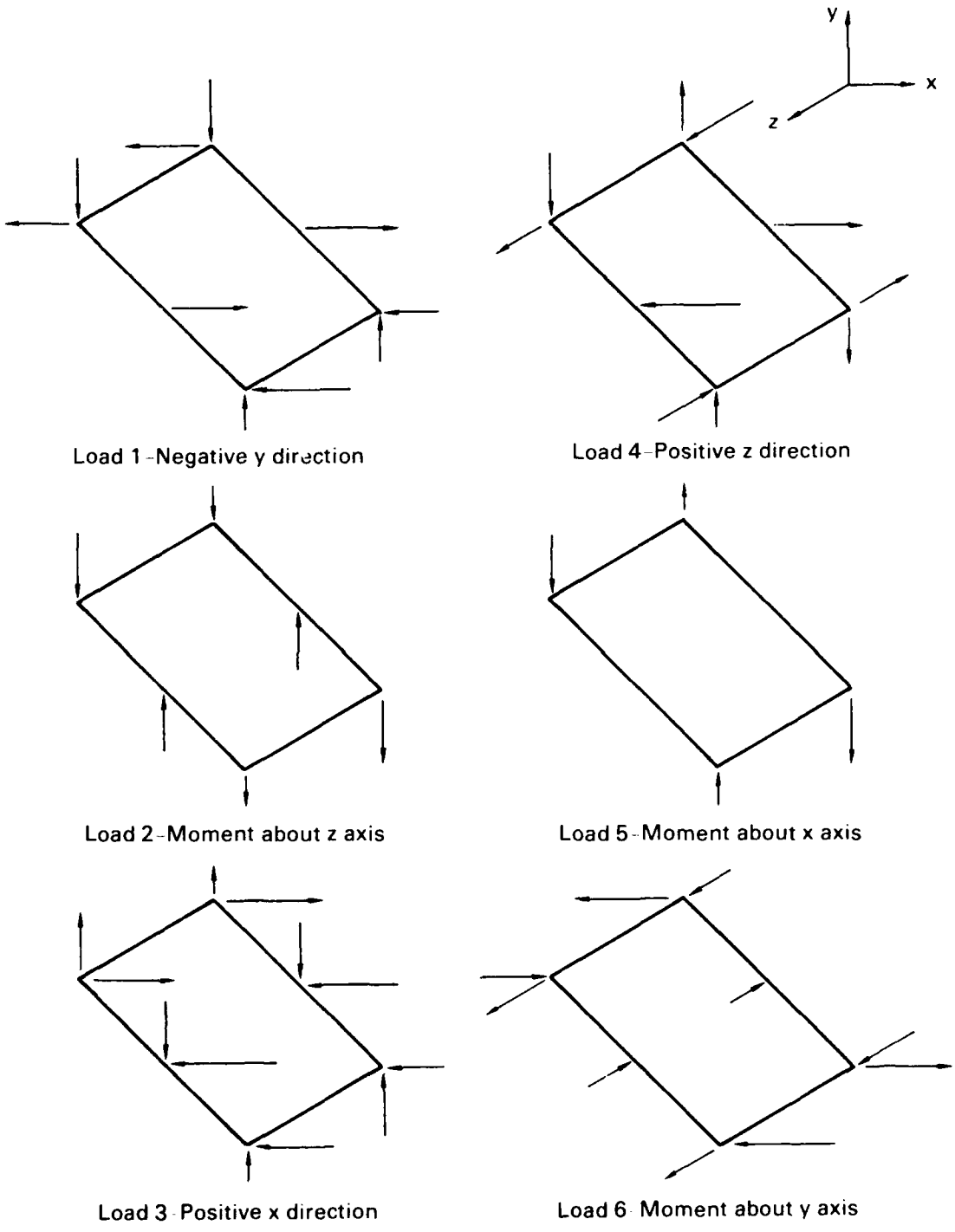

Figure 31. Summary of reaction forces.

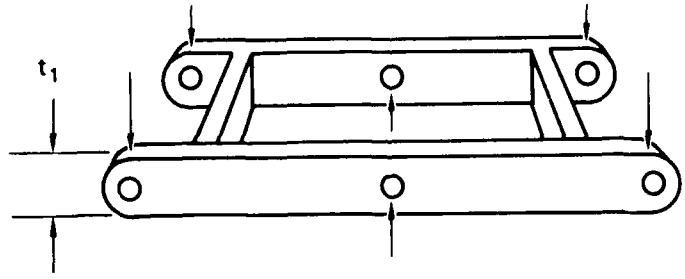

a.

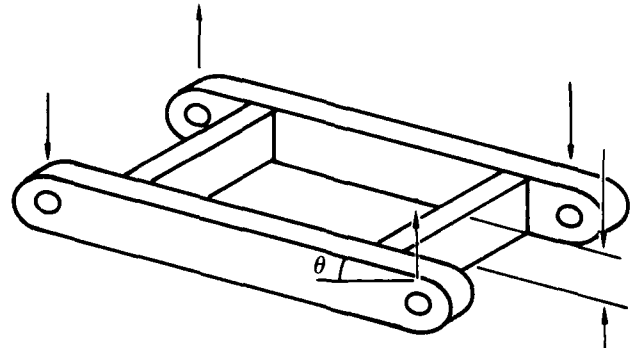

b.

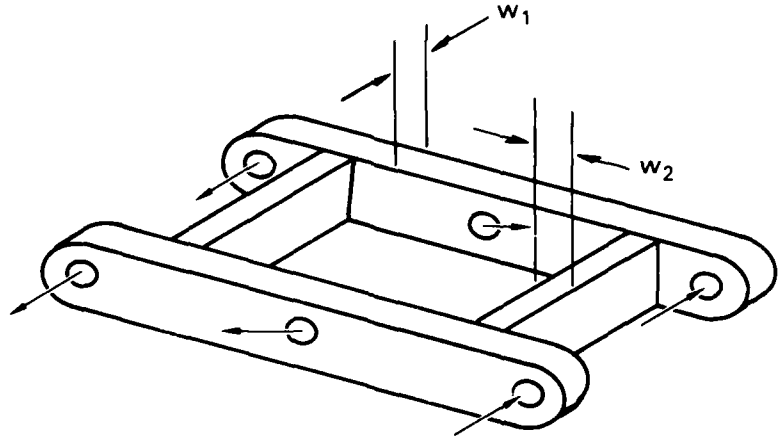

c.

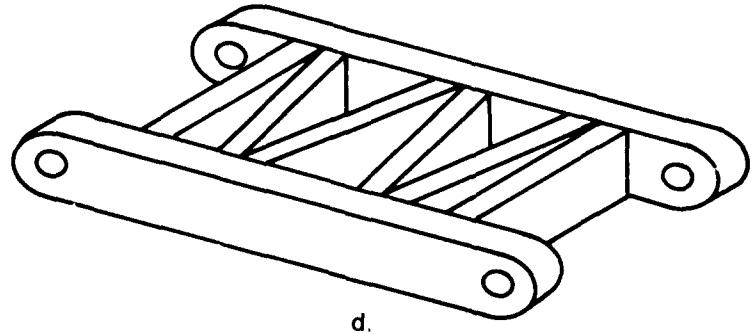

d.

Figure 32. Crossbracing.

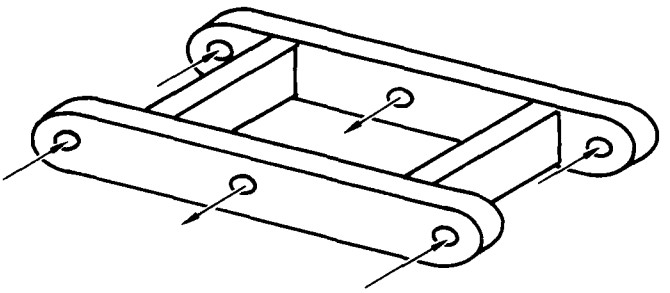

e.

Figure 32. Crossbracing (continued).

7.0 CONCLUSION

The purpose of this paper was to derive general equations for calculating reaction forces throughout a scissor lift. In order to derive these equations, two critical observations were made. The first observation was that the reaction forces in the scissor members outside of the levels containing the actuator are completely unaffected by the orientation of the actuator. This allows the scissor members above the actuator and the members below the actuator to be modelled as two "basic scissor structures," a scissor structure that is pinned to ground at all four bottom joints and that contains no actuators. The second critical observation was that if the lift is assumed to be frictionless, then the principal of conservation of energy applies that states that work in equals work out. This principal allows the actuator forces to be calculated directly.

In the first part of the paper, reaction force equations were derived for the basic scissor structure. In this derivation, the friction at the joints was assumed to be negligible. Next, equations for determining the actuator forces were derived using the principal of conservation of energy. Following these derivations, the proper application of these equations in determining the reaction forces throughout the lift was given. Finally, several design issues were discussed. These issues included actuator placement and "strength and rigidity."

8.0 BIBLIOGRAPHY

Fulks, W. 1978. *Advanced Calculus*, John Wiley and Sons, Inc., Toronto, Canada.

Levinson, I.J. 1971. *Statics and Strengths of Materials*, Prentice Hall Inc., Englewood Cliffs, NJ.

Solorzano, M.R. 1989. "TOV Surveillance Lift Configurations," Memo 535-12/89, Naval Ocean Systems Center, San Diego, CA.

Solorzano, M.R. 1989. "TOV Surveillance Systems Stability Testing," Memo 535-36/89. Naval Ocean Systems Center, San Diego, CA.

SUPPLEMENTARY

INFORMATION

ERRATA

NAVAL OCEAN SYSTEMS CENTER
SAN DIEGO, CALIFORNIA 92152-5000

20 December 1990

AD-A225220

NOSC Technical Document 1550
Mathematical Analysis of Scissor Lifts
By H. M. Spackman
Dated June 1988

Literature Change

1. Replace the covers and the Form 1473 with the attached corrected copies. The documents were mailed to you 6 August 1990.

Naval Ocean Systems Center
San Diego, CA 92152-5000

Technical Document 1550
August 1990

Mathematical Analysis of Scissor Lifts

H. M. Spackman

NAVAL OCEAN SYSTEMS CENTER
San Diego, California 92152–5000

E. G. SCHWEIZER, CAPT, USN
Commander

R. M. HILLYER
Technical Director

ADMINISTRATIVE INFORMATION

This work was performed for the U.S. Marine Corps, Development/Education Command, Quantico, VA 22134, under program element number 0603635M and agency accession number DN308 274. The work was performed by the Advanced Technology Development Branch, Code 612, Naval Ocean Systems Center, San Diego, CA 92152–5000.

Released by
R. E. Glass, Head
Advanced Technology
Development Branch

Under authority of
D. W. Murphy, Head
Advanced Systems
Division

FS

UNCLASSIFIED

SECURITY CLASSIFICATION OF THIS PAGE

REPORT DOCUMENTATION PAGE

1a. REPORT SECURITY CLASSIFICATION UNCLASSIFIED	1b. RESTRICTIVE MARKINGS
2a. SECURITY CLASSIFICATION AUTHORITY	3. DISTRIBUTION/AVAILABILITY OF REPORT Approved for public release; distribution is unlimited.
2b. DECLASSIFICATION/DOWNGRADING SCHEDULE	
4. PERFORMING ORGANIZATION REPORT NUMBER(S) NOSC TD 1550	5. MONITORING ORGANIZATION REPORT NUMBER(S)
6a. NAME OF PERFORMING ORGANIZATION Naval Ocean Systems Center 6b. OFFICE SYMBOL (if applicable) Code 612	7a. NAME OF MONITORING ORGANIZATION
6c. ADDRESS (City, State and ZIP Code) San Diego, CA 92152-5000	7b. ADDRESS (City, State and ZIP Code)
8a. NAME OF FUNDING/SPONSORING ORGANIZATION U.S. Marine Corps 8b. OFFICE SYMBOL (if applicable)	9. PROCUREMENT INSTRUMENT IDENTIFICATION NUMBER N66001-85-C-0205
8c. ADDRESS (City, State and ZIP Code) Development/Education Command Quantico, VA 22134	10. SOURCE OF FUNDING NUMBERS PROGRAM ELEMENT NO.: 0603635M PROJECT NO.: CH58 TASK NO.: AGENCY ACCESSION NO.: DN308274

11. TITLE (include Security Classification)
MATHEMATICAL ANALYSIS OF SCISSOR LIFTS

12. PERSONAL AUTHOR(S)
H. M. Spackman

13a. TYPE OF REPORT	13b. TIME COVERED	14. DATE OF REPORT (Year, Month, Day)	15. PAGE COUNT
Final	FROM TO	August 1990	63

16. SUPPLEMENTARY NOTATION

17. COSATI CODES			18. SUBJECT TERMS (Continue on reverse if necessary and identify by block number)
FIELD	GROUP	SUB-GROUP	scissor lift actuator placement member cross-section

19. ABSTRACT (Continue on reverse if necessary and identify by block number)

This document presents mathematical techniques for analyzing reaction forces in scissor lifts. It also presents several design issues including actuator placement, member cross-section, and rigidity.

20. DISTRIBUTION/AVAILABILITY OF ABSTRACT	21. ABSTRACT SECURITY CLASSIFICATION	
☒ UNCLASSIFIED/UNLIMITED ☐ SAME AS RPT ☐ DTIC USERS	UNCLASSIFIED	
22a. NAME OF RESPONSIBLE PERSON H. M. Spackman	22b. TELEPHONE (include Area Code) (808) 553-6110	22c. OFFICE SYMBOL Code 612

DD FORM 1473, 84 JAN

83 APR EDITION MAY BE USED UNTIL EXHAUSTED
ALL OTHER EDITIONS ARE OBSOLETE

UNCLASSIFIED

SECURITY CLASSIFICATION OF THIS PAGE